Adaptive methods for time-modulated stars

Giovanni Motta & Darlin Soto

Center for Astrophysics, Harvard & Smithsonian

3-3-2020

Outline

Periodic modulated variable stars

Modulated luminosity of variabler stars

- Amplitude modulation
- Angle modulation

Estimation

- Semi-parametric approach
- Simulation Results
- An application

Non-periodic modulated variable stars

ARMA modeling

- CARMA(p, q) process
- Locally stationary processes

Estimation

- Semi-parametric approach
- Simulation Results
- An application

Modulated means *slowly* time-varying

- Target: variable stars characterized by *time-modulated*
  i.e. *slowly time-varying* parameters: mean, amplitude, period and phase.

- Goals: modeling and forecasting light curves of these variable stars using time series models.

- Variable stars

1) Periodic: Long-Period-Variable and Blazhko,
2) Non-periodic: Galaxies (AGN)

LPV stars: Miras

- Average period of 100 to 1,000 days with large amplitudes of light variation of more than 2.5 magnitudes visually and more than 1 magnitude in the infrared wavelengths.
- The period is a very important parameter as indicator of their size and luminosity as well as their age, mode of pulsation and their overall evolution.
- Research revealed important correlations between the period and (i) amplitude, (ii) mass loss (iii) IR excess due to dust surrounding the star.
- Period & shape of the light curve (Mattei, 1997):

- periods < 200 days: symmetrical light curves and smaller amplitudes;
- periods > 200 days: larger amplitudes & steeper rising branches of the curve;
- periods > 300 days: quite large amplitudes with standstills or humps in the ascending branches of their light curves.

LPV stars: Extreme Miras

Miras at the ends of the ranges in periods and amplitudes

- V369 Cyg is an example of LPV star;
- the maximum amplitude is relatively high at up to 5 magnitudes.

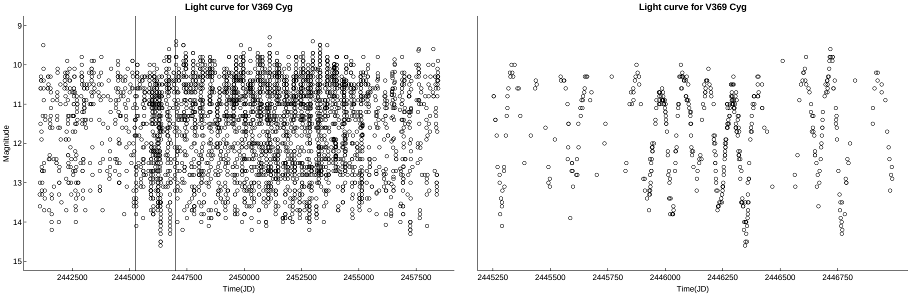

Left: all the observations. Right: 1,500 day interval centered around 1985 (the star was well observed throughout a number of cycles). From AAVSO.

LPV stars: Extreme Miras

Miras at the ends of the ranges in periods and amplitudes

- Mira LPV 32697 is another example of LPV star;
- its magnitude exhibits a (possibly quadratic) time-varying mean, as well as time-varying amplitude and period.

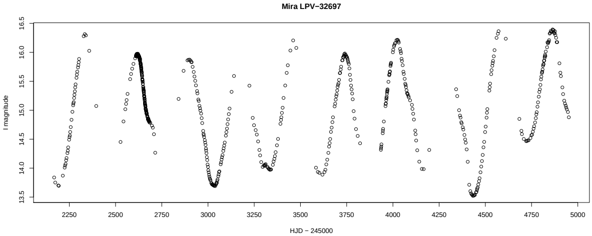

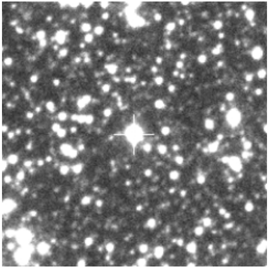

Left: 616 observations. Right: Finding chart (60x60 arcsec). From OGLE.

The Blazhko effect: long-period modulation

- It is a variation in period, amplitude or phase in RR Lyrae variable stars.
- It was first observed by Blazhko (1907) in the star RW Draconis.
- The amplitude-modulated pulsation of RR Lyrae stars has a strong periodic component with an often observed variation on a longer time scale.
- The RR Lyr's primary period has shown small increases and decreases since its discovery in 1901.
- The Blazhko effect is a periodic amplitude and/or phase modulation shown by some 20-30% of the galactic RRab stars.

The Blazhko effect: long-period modulation

These stars have pulsation periods of about half a day.

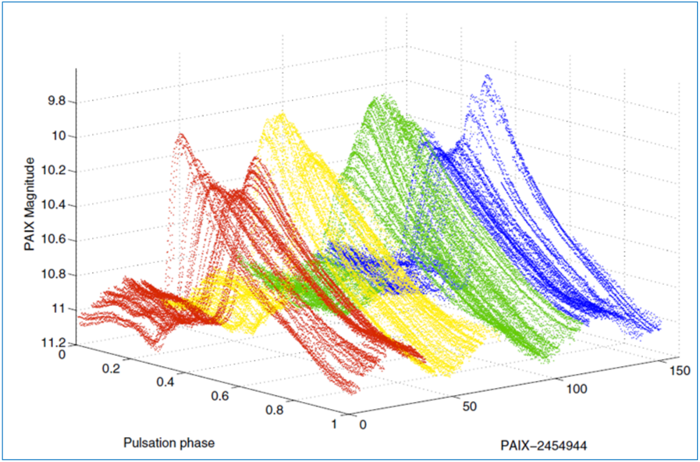

Chadid et al. (2014, AJ, 148, 88)

The Blazhko effect: long-period modulation

The amplitude variation is accompanied by phase changes of the same period.

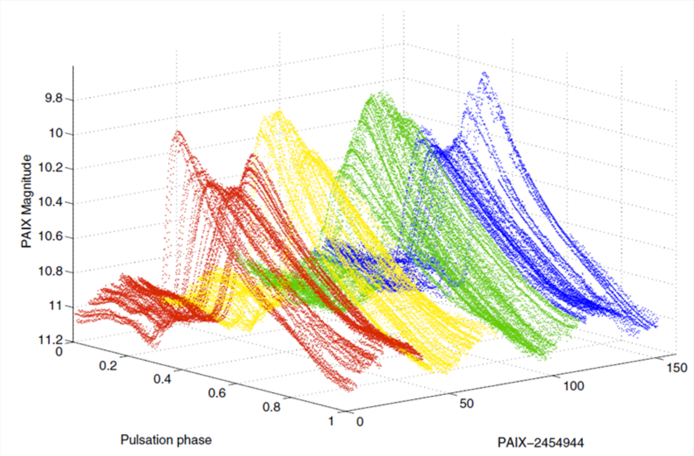

Chadid et al. (2014, AJ, 148, 88)

The Blazhko effect: long-period modulation

The modulation can be anywhere between 10 and 700 days.

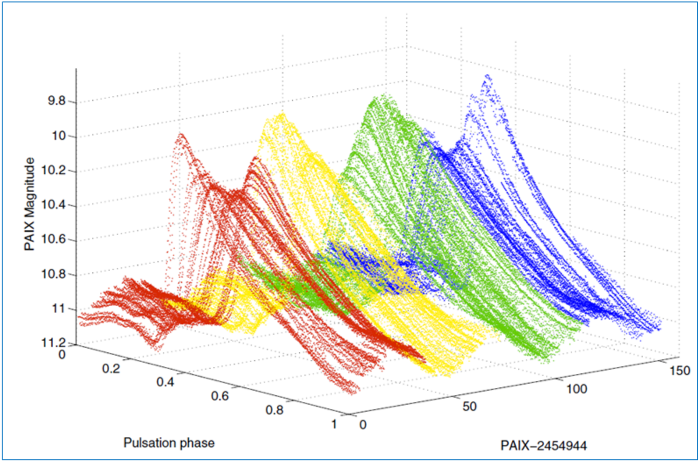

Chadid et al. (2014, AJ, 148, 88)

The Blazhko effect: long-period modulation

Any correlation between the modulation and the fundamental period.

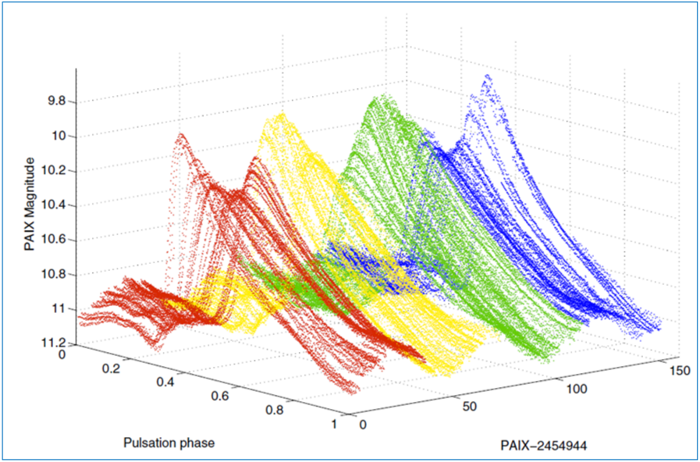

Chadid et al. (2014, AJ, 148, 88)

The Blazhko effect: long-period modulation

No regularity can be found in the changes of the primary period.

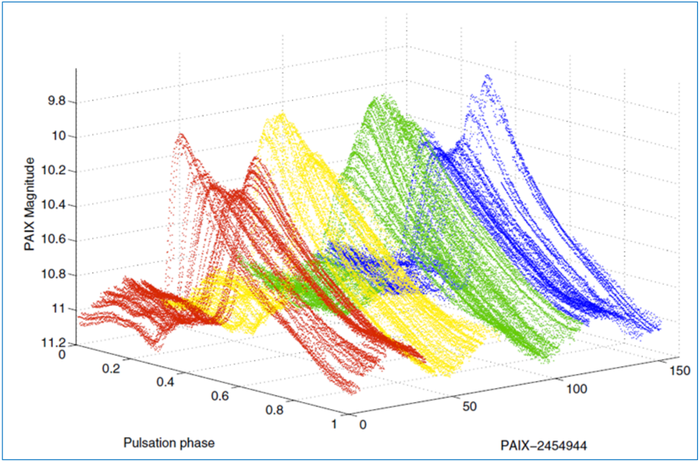

Chadid et al. (2014, AJ, 148, 88)

The Blazhko effect: long-period modulation

Both amplitude and length of the secondary period seems to be variable.

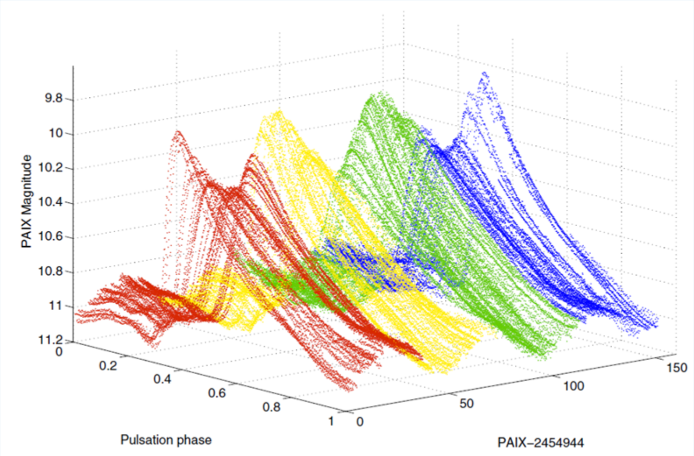

Chadid et al. (2014, AJ, 148, 88)

The Blazhko effect: long-period modulation

from Kolenberg (2006)

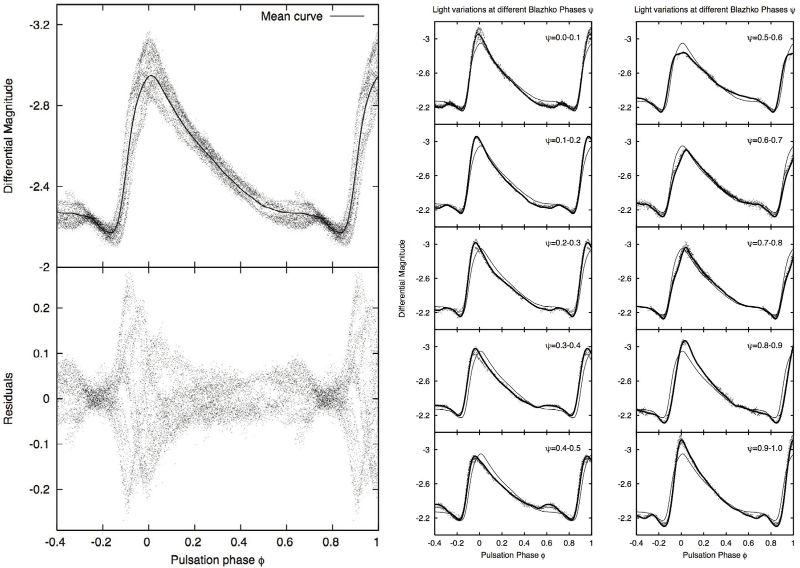

The Blazhko effect: long-period modulation

from Kolenberg (2006)

Left-Top

- Combined RR Lyr V data folded with the main pulsation period $f_0 = 1.76$.
- The mean light curve is defined by the components of the fit, varying with only f_0 and its 10 significant harmonics (up to 11 f_0).

Left-Bottom

- Residuals after subtraction of the mean light curve.

There is an interval in the pulsation cycle (right after the phase of the so-called bump), roughly $\phi = 0.72 - 0.82$, during which the star's intensity barely changes over the Blazhko cycle.

The Blazhko effect: long-period modulation

from Kolenberg (2006)

Right

10 consecutive phase intervals in the Blazhko cycle of about 39 days, e.g.:
$\psi = 0.0 - 0.1$, $\psi = 0.1 - 0.2$, etc., where
Blazhko phase $\psi = 0$ is the phase of maximum Blazhko amplitude.

- Thick solid lines: pulsation light curves constructed from the data (dots) falling into the 0.1 phase intervals of the Blazhko cycle.
- Full line: mean light curve derived from all data.
- Thin line: mean light curve over all Blazhko phase intervals.

The Blazhko effect: long-period modulation

from Kolenberg (2006)

Right

10 consecutive phase intervals in the Blazhko cycle of about 39 days, e.g.:
$\psi = 0.0 - 0.1$, $\psi = 0.1 - 0.2$, etc., where
Blazhko phase $\psi = 0$ is the phase of maximum Blazhko amplitude.

- Thick solid lines: pulsation light curves constructed from the data (dots) falling into the 0.1 phase intervals of the Blazhko cycle.
- Full line: mean light curve derived from all data.
- Thin line: mean light curve over all Blazhko phase intervals.

Certain features in the light curve occur at specific phase intervals in the Blazhko cycle. Studying their origin and modeling those changes can bring us closer to understanding the modulation.

The Blazhko effect: long-period modulation

from Kolenberg (2006)

Right

10 consecutive phase intervals in the Blazhko cycle of about 39 days, e.g.:
$\psi = 0.0 - 0.1$, $\psi = 0.1 - 0.2$, etc., where
Blazhko phase $\psi = 0$ is the phase of maximum Blazhko amplitude.

- Thick solid lines: pulsation light curves constructed from the data (dots) falling into the 0.1 phase intervals of the Blazhko cycle.
- Full line: mean light curve derived from all data.
- Thin line: mean light curve over all Blazhko phase intervals.

The strong amplitude and phase modulation in RR Lyr is accompanied by changes in the shape (and position) of the bump, and the hump is only observed at certain Blazhko phases.

The Blazhko effect: long-period modulation

from Benkő et al. (2018)

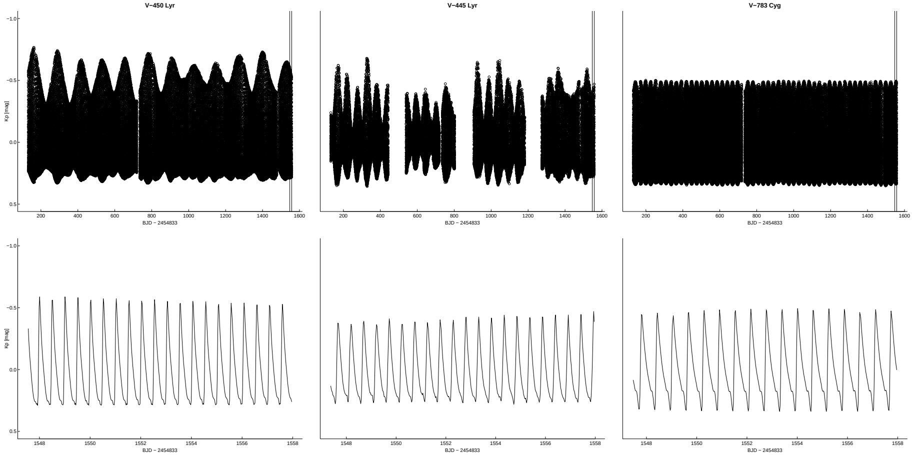

V-450 Lyr V-445 Lyr V-783 Cyg

The Blazhko effect: long-period modulation

from Benkő et al. (2018)

The amplitude modulation is fairly nonsinusoidal which is evident from the envelopes of the corresponding light curves in the figure.

- V783 Cyg
  Carefully investigating we detect small differences between consecutive cycles.

- V445 Lyr
  - The light curve of the star shows strong and complicated amplitude changes.
  - The parameters (periods, amplitudes and phases) are heavily varying.

- V450 Lyr
  - The shape of the maxima curve of V450 Lyr suggests a strong beating phenomenon between two modulation periods.
  - The authors fit a quadratic function to the O-C diagram of this stars.

The Blazhko effect: long-period modulation

from Guggenberger et al. (2011)

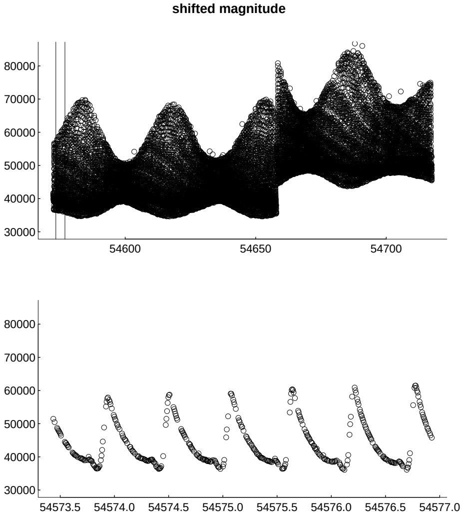

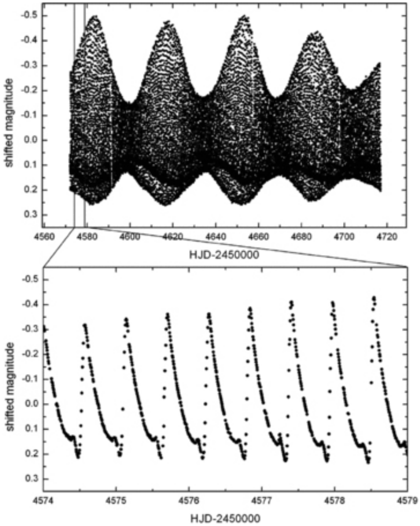

The Blazhko effect: long-period modulation

from Guggenberger et al. (2011)

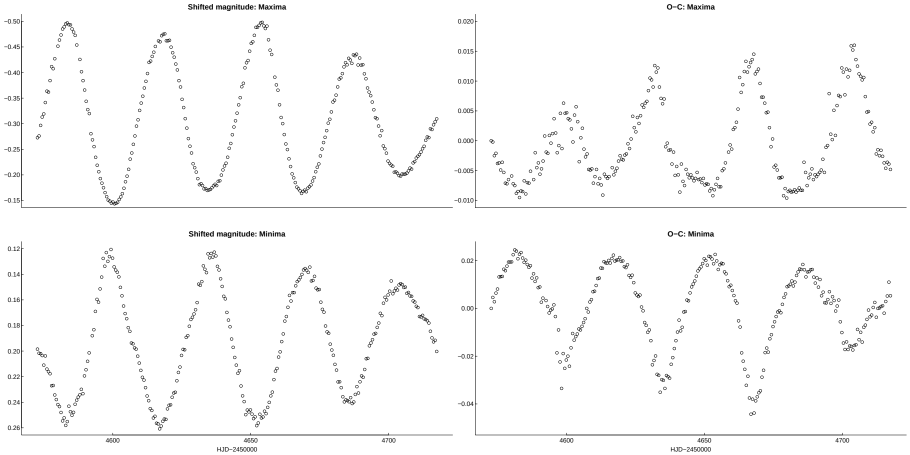

We observe strong changes in the Blazhko modulation, both in brightness and O-C variations.

The Blazhko effect: long-period modulation

from Guggenberger et al. (2011)

Model fitted to the data of CoRoT ID 105288363

$$
\begin{aligned}
f(t) &= A_0 + \sum_{k=1}^{K} \{ A_k \sin\left(2\pi(kf_0 t + \varphi_k)\right) \\
&+ \sum_{m=1}^{2} B_{km}^{(1)} \sin\left(2\pi[(kf_0 + mf_B)t + \varphi_{km}^{(1)}]\right) + \sum_{m=1}^{2} B_{km}^{(2)} \sin\left(2\pi[(kf_0 - mf_B)t + \varphi_{km}^{(2)}]\right)\} \\
&+ B_0 \sin\left(2\pi[f_B t + \varphi_B]\right)
\end{aligned}
$$

- f_B is the Blazhko frequency,
- $B_{k1}^{(1)}$ and $B_{k1}^{(2)}$ are the amplitudes of the triplet components
- $B_{k2}^{(1)}$ and $B_{k2}^{(2)}$ are the amplitudes of the quintuplet peaks on the higher and lower sides of the main pulsation component
- B_0 is the amplitude of the Blazhko frequency itself.

The Blazhko effect: long-period modulation

from Guggenberger et al. (2011)

Model fitted to the data of CoRoT ID 105288363

$$
\begin{aligned}
f(t) \quad &= \quad A_0 + \sum_{k=1}^{K} \{ A_k \sin\left(2\pi(kf_0 t + \varphi_k)\right) \\
&+ \quad \sum_{m=1}^{2} B_{km}^{(1)} \sin\left(2\pi[(kf_0 + mf_B)t + \varphi_{km}^{(1)}]\right) + \sum_{m=1}^{2} B_{km}^{(2)} \sin\left(2\pi[(kf_0 - mf_B)t + \varphi_{km}^{(2)}]\right) \} \\
&+ \quad B_0 \sin\left(2\pi[f_B t + \varphi_B]\right)
\end{aligned}
$$

This is the standard method of fitting the light curves of Blazhko RR Lyrae stars, assuming equidistant triplets, extended here to include also equidistant quintuplets and the Blazhko frequency itself.

The Blazhko effect: long-period modulation

Benkő (2017)

Non-sinusoidally modulated model for the RR Lyrae light

$$m(t) = [a_0^A + g^A(t)]\{a_0 + \sum_{i=1}^{n} a_1 \sin[2\pi \mathrm{i} f_0 t + \varphi_i + \mathrm{i} g^F(t)]\} \qquad (1)$$

where the modulation functions are

$$g^M(t) = \sum_{j=1}^{\ell_M} a_j^M \sin\left(2\pi j f_m t + \varphi_j^M\right), \qquad M = A \text{ or } F.$$

- f_0 and f_m are the main pulsation and the modulation frequencies,
- a and φ are the Fourier amplitudes and phases, respectively.
- The a_0^A , a_0 are the zero point constants;
- n and ℓ_M are the number of terms in the finite Fourier sums.
- A indicates the amplitude modulation (AM) and F means the frequency modulation (FM).

The Blazhko effect: long-period modulation

Benkő (2017)

Non-sinusoidally modulated model for the RR Lyrae light

$$m(t) = [a_0^A + g^A(t)]\{a_0 + \sum_{i=1}^{n} a_1 \sin[2\pi \mathrm{i} f_0 t + \varphi_i + \mathrm{i} g^F(t)]\} \tag{1}$$

where the modulation functions are

$$g^M(t) = \sum_{j=1}^{\ell_M} a_j^M \sin\left(2\pi j f_m t + \varphi_j^M\right), \qquad M = A \text{ or } F.$$

- Model (1) says that the Blazhko light curves are not modulated signals but signals of a different and more complicated physical effect.
- These represent the non-sinusoidal nature of the light curves but they have no physical meaning.

The Blazhko effect: long-period modulation

Benkő (2017)

Non-sinusoidally modulated model for the RR Lyrae light

$$m(t) = [a_0^A + g^A(t)]\{a_0 + \sum_{i=1}^{n} a_1 \sin[2\pi \mathrm{i} f_0 t + \varphi_i + \mathrm{i} g^F(t)]\} \qquad (1)$$

where the modulation functions are

$$g^M(t) = \sum_{j=1}^{\ell_M} a_j^M \sin\left(2\pi j f_m t + \varphi_j^M\right), \qquad M = A \text{ or } F.$$

- Though model (1) allows for time-varying parameters, the coefficients $g(t)$ follow a parametric specification.
- In contrast, we want to allow the coefficients to be fully non-parametric and thus adaptive.

Outline

Modulation

Continuous wave modulation can be divided into two sets:

- amplitude modulation (AM)
- angle modulation
  - frequency modulation (PM)
  - phase modulation (FM)

Outline

Amplitude modulation

- Carrier wave $c(t) = U_c \sin(2\pi f_c t + \phi_c)$
where U_c, f_c, and ϕ_c are the amplitude, frequency, and phase of the carrier wave, respectively.

- Modulation signal $U_m(t)$: waveform (the message) to be transmitted

- Modulated signal

$$\begin{aligned} U_{AM}(t) &= [U_c + U_m(t)] \sin(2\pi f_c t + \phi_c) \\ &= \left[1 + \frac{U_m(t)}{U_c}\right] c(t) \end{aligned} \tag{2}$$

Amplitude modulation: Example 1

- Carrier wave $c(t) = U_c \sin(2\pi f_c t + \phi_c)$

- Modulation signal $U_m(t) = U_m^A \sin(2\pi f_m t + \phi_m^A)$

- Modulated signal

$$U_{AM}(t) = [U_c + U_m^A \sin(2\pi f_m t + \phi_m^A)] \sin(2\pi f_c t + \phi_c),$$

or equivalently, using

$$\sin(a)\sin(b) = \tfrac{1}{2}[\cos(a-b) - \cos(a+b)] \quad \text{and} \quad \sin(a) = \cos(a - \tfrac{\pi}{2})$$

$$\begin{aligned} U_{AM}(t) = {} & U_c \sin(2\pi f_c t + \phi_c) \\ & + \frac{U_m^A}{2}\left[\sin(2\pi(f_m - f_c) + (\phi_m^A - \phi_c + \frac{\pi}{2}))\right] \\ & - \frac{U_m^A}{2}\left[\sin(2\pi(f_m + f_c) + (\phi_m^A + \phi_c + \frac{\pi}{2}))\right] \end{aligned}$$

Amplitude modulation: Example 2

a generalization of Example 1

$$c(t) = a_0 + \sum_{k=1}^{K} a_k \sin(2\pi k f_0 t + \phi_k), \tag{3}$$

$$U_m(t) = U_m^A \sin(2\pi f_m t + \phi_m^A). \tag{4}$$

Substituting equations (3) and (4) into (2) we have

$$U_{AM}(t) = \left[1 + \frac{U_m^A \sin(2\pi f_m t + \phi_m^A)}{U_c}\right] \left[a_0 + \sum_{k=1}^{K} a_k \sin(2\pi k f_0 t + \phi_k)\right]. \tag{5}$$

If we call $h = U_m^A / U_c$, and using the same identities, expression (5) becomes

$$\begin{aligned} U_{AM}(t) = a_0 &+ \sum_{k=1}^{K} a_k \sin(2\pi k f_0 t + \phi_k) + a_0 h \sin(2\pi f_m t + \phi_m^A) \\ &+ \sum_{k=1}^{K} \frac{a_k h}{2} \sin(2\pi(k f_0 - f_m)t + (\phi_k - \phi_m) + \pi/2) \\ &- \sum_{k=1}^{K} \frac{a_k h}{2} \sin(2\pi(k f_0 + f_m)t + (\phi_k + \phi_m) + \pi/2). \end{aligned}$$

Amplitude modulation: Example 3

Sama $c(t)$ as in Example 2, and (2) is

$$\left[1 + \frac{U_m(t)}{U_c}\right] = a_0^A + \sum_{p=1}^{q} a_p^A \sin(2\pi p f_m t + \phi_p^A), \tag{6}$$

where $a_0^A = 1 + a_0^m/U_c$, and $a_p^A = a_p^m/U_c$. Substituting (3) and (6) into (2)

$$U_{AM}(t) = \left[a_0^A + \sum_{p=1}^{q} a_p^A \sin(2\pi p f_m t + \phi_p^A)\right]\left[a_0 + \sum_{k=1}^{K} a_k \sin(2\pi k f_0 t + \phi_k)\right]. \tag{7}$$

Using $\sin(a)\sin(b)$ as above, $\sin(a+\pi/2) = \cos(a)$, and $\sin(a-\pi/2) = -\cos(a)$,

$$U_{AM}(t) = \sum_{p=0}^{q}\sum_{k=0}^{n} \frac{a_p^A a_k}{2} \sin(2\pi[kf_0 \pm pf_m]t \pm \phi_{kp}^{\pm}),$$

with $\phi_{kp}^+ = \phi_k + \phi_p^A - \pi/2$, $\phi_{kp}^- = \phi_k - \phi_p^A + \pi/2$, and $\phi_0^A = \phi_0 = \pi/2$.

Amplitude modulation: Example 3 (continued)

A more complicated form of the carrier wave is

$$c(t) = U_{c1} \sin(2\pi f_{c1} t + \phi_{c1}) + U_{c2} \cos(2\pi f_{c2} t + \phi^*_{c2}). \tag{8}$$

Using the basic trigonometrical identity $\sin(a) = \cos(a - \frac{\pi}{2})$, equation (8) can be seen as a sinusoidal wave with two harmonics, that is,

$$c(t) = U_{c1} \sin(2\pi f_{c1} t + \phi_{c1}) + U_{c2} \sin(2\pi f_{c2} t + \phi_{c2}). \tag{9}$$

where $\phi_{c2} = \phi^*_{c2} + \frac{\pi}{2}$. Substituting the equation (9) into (2) we have

$$U_{AM}(t) = \left[1 + \frac{U_m(t)}{U^*_c}\right] \left[\sum_{i=1}^{2} U_{ci} \sin(2\pi f_{ci} t + \phi_{ci})\right].$$

where U^*_c is the amplitude of the non-modulated curve $c(t)$.

Amplitude modulation: Example 4

Suppose $U_{c1} = U_{c2} = U_c$, then the carrier wave (9) is given by

$$c(t) = U_c \sin(2\pi f_{c1} t + \phi_{c1}) + U_c \sin(2\pi f_{c2} t + \phi_{c2}). \tag{10}$$

Using $\sin(a) + \sin(b) = 2\cos(\frac{a-b}{2})\sin(\frac{a+b}{2})$,

$$c(t) = \underbrace{\left[2U_c \cos\left(2\pi \frac{(f_{c1} - f_{c2})}{2} t + \frac{\phi_{c1} - \phi_{c2}}{2}\right)\right]}_{[U_c(t) = time-varying\ \ amplitude]} \underbrace{\sin\left(2\pi \frac{(f_{c1} + f_{c2})}{2} t + \frac{\phi_{c1} + \phi_{c2}}{2}\right)}_{average\ \ wave}$$

If $U_m(t) = U_m^A \sin(2\pi f_m t + \phi_m^A)$, the modulated signal $U_{AM}(t)$ is as follows

$$U_{AM}(t) = [U_c(t) + U_m^A \sin(2\pi f_m t + \phi_m^A)] \sin\left(2\pi \frac{(f_{c1} + f_{c2})}{2} t + \frac{\phi_{c1} + \phi_{c2}}{2}\right),$$

or in form of equation (2) we have

$$U_{AM}(t) = \left[1 + \frac{U_m^A \sin(2\pi f_m t + \phi_m^A)}{U_c(t)}\right] \left[U_c \sum_{i=1}^{2} \sin(2\pi f_{ci} t + \phi_{ci})\right],$$

where $U_c(t)$ is the amplitude of the non-modulated curve $c(t)$.

Outline

Phase modulation

The phase modulation (PM) changes the phase angle of the carrier signal. We assume the sinusoidal carrier wave to be

$$c(t) = U_c \sin(\Theta(t)), \tag{11}$$

and $\Theta(t) = 2\pi f_c t + \phi_c$ represents the angle part of the function. Suppose that the modulating is $U_m(t)$, then $\Theta(t) = 2\pi f_c t + [\phi_c + U_m(t)]$, and the modulated signal is given by

$$U_{PM}(t) = U_c \sin(2\pi f_c t + [\phi_c + U_m(t)]).$$

The instantaneous frequency of the modulated signal, $U_{PM}(t)$, is

$$f(t) = \frac{\partial\Theta(t)}{\partial t} = 2\pi f_c + \frac{\partial U_m(t)}{\partial t}. \tag{12}$$

Frequency modulation

The frequency modulation (FM) varies the carrier frequency using the modulating signal $U_m(t)$. Now, we assume that $\Theta(t) = 2\pi f(t)t + \phi_c$, where $f(t)$ is the instantaneous frequency which is modulated by the signal $U_m(t)$ as

$$f(t) = 2\pi f_c + U_m(t). \tag{13}$$

From fundamental Theorem of Calculus, we can express (12) as

$$\Theta(t) = \int_0^t f(\tau) d\tau.$$

Substituting (13) in the above expression we obtain

$$\Theta(t) = 2\pi f_c t + \int_0^t U_m(\tau) d\tau.$$

Finally, using the same carrier wave (11), the frequency modulation signal is

$$U_{FM}(t) = U_c \sin(2\pi f_c t + \int_0^t U_m(\tau) d\tau + \phi_c). \tag{14}$$

Frequency modulation: Example 5

A simple case: $\int_0^t U_m(\tau)d\tau$ takes the form

$$\int_0^t U_m(\tau)d\tau = \sin(2\pi f_m t + \phi_c^F). \tag{15}$$

Substituting (15) in (14), the modulated signal is

$$U_{FM}(t) = U_c \sin(2\pi f_c t + \sin(2\pi f_m t + \phi_c^F) + \phi_c).$$

Examples 1 & 4 (AM) and 5 (FM)

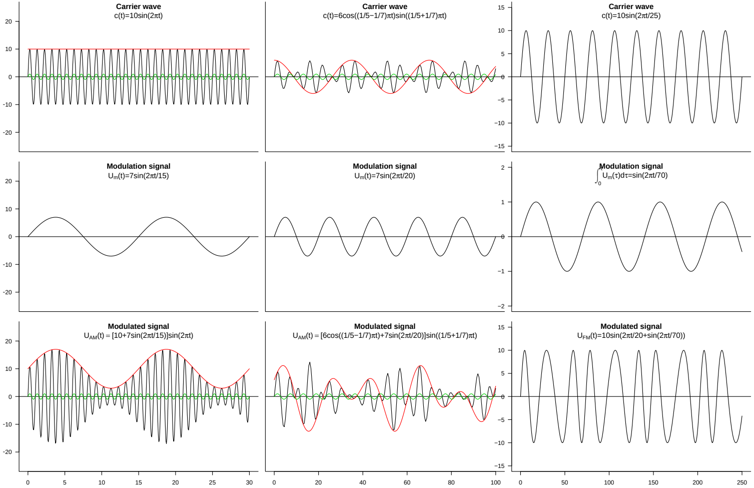

Sinusoidal signal: black; its amplitude: red; its wave: green.

Smoothly-varying parameters

Data:

- random observed vector $\boldsymbol{Y} = (Y_1, Y_2, \ldots, Y_N)'$
- time vector $\boldsymbol{t} = (t_1, t_2, \ldots, t_N)'$

Modulation model

$$Y_i = m(t_i) + \sum_{k=1}^{K} \{g_{1k}(t_i)\cos(w_k t_i) + g_{2k}(t_i)\sin(w_k t_i)\} + X_i, \qquad i = 1, \ldots, N,$$

- smooth trend
- smooth time-varying amplitudes
- K number of harmonics
- $\boldsymbol{X} = (X_1, \ldots, X_N)'$ are values of a causal zero-mean ARMA(p,q) process

$$\phi(L)X_i = \theta(L)Z_i, \qquad \{Z_i\} \sim WN(0, \sigma_Z^2),$$

Outline

Estimation

- The basis matrix formed by B-splines

$$\mathbf{B} = \begin{pmatrix} B_1(t_1) & B_2(t_1) & \dots & B_J(t_1) \\ B_1(t_2) & B_2(t_2) & \dots & B_J(t_2) \\ B_1(t_3) & B_2(t_3) & \dots & B_J(t_3) \\ \vdots & \vdots & \ddots & \vdots \\ B_1(t_N) & B_2(t_N) & \dots & B_J(t_N) \end{pmatrix}$$

  of dimension $N \times J$, where J depends on the number of knots and the degree of the B-spline.

- $m(t_i) = \sum_{j=1}^{J} \alpha_j B_j(t_i)$

- $g_{1k}(t_i) = \sum_{j=1}^{J} \beta_{kj} B_j(t_i)$, $k = 1, \dots, K$

- $g_{2k}(t_i) = \sum_{j=1}^{J} \gamma_{kj} B_j(t_i)$, $k = 1, \dots, K$

Estimation: splines regression

In matrix notation

$$\boldsymbol{m} = \mathbf{B}\boldsymbol{\alpha}, \quad \boldsymbol{g}_{1k} = \mathbf{B}\boldsymbol{\beta}_k \text{ and } \boldsymbol{g}_{2k} = \mathbf{B}\boldsymbol{\gamma}_k, \qquad k = 1, \ldots, K$$

$$\mathbf{C}_k = \operatorname{diag}\{\cos(w_k t_1), \ldots, \cos(w_k t_N)\}, \qquad k = 1, \ldots, K$$

$$\mathbf{S}_k = \operatorname{diag}\{\sin(w_k t_1), \ldots, \sin(w_k t_N)\}, \qquad k = 1, \ldots, K$$

Model for the expected value

$$\mathbb{E}(\boldsymbol{Y}) = \mathcal{B}\boldsymbol{\theta},$$

$\mathcal{B} = [\mathbf{B}|\mathbf{C}_1\mathbf{B}|\mathbf{S}_1\mathbf{B}|\ldots|\mathbf{C}_K\mathbf{B}|\mathbf{S}_K\mathbf{B}]$ of dimension $N \times c$, $\quad c = J(2K+1)$

$\boldsymbol{\theta} = (\alpha, \beta_1, \gamma_1, \ldots, \beta_K, \gamma_K)'$ of dimension $c \times 1$

Estimation: B-splines

Minimizing the function of $\boldsymbol{\theta}$

$$M_{\boldsymbol{\theta}} = ||\mathbf{T}\boldsymbol{Y} - \mathbf{T}\mathcal{B}\boldsymbol{\theta}||^2,$$

where $\mathbf{T}$ is $N \times N$ satisfying $\mathbf{T}^{'}\mathbf{T} = \sigma_{X}^2 \boldsymbol{\Gamma}_{X}^{-1}$, with

$$\sigma_{X}^2 = \mathbb{V}\mathrm{ar}(\boldsymbol{X}), \qquad \text{and} \qquad \boldsymbol{\Gamma}_{X} = \mathbb{E}(\boldsymbol{X}\boldsymbol{X}^{'})$$

The least square solution is

$$\hat{\boldsymbol{\theta}} = (\mathcal{B}^{'}\boldsymbol{\Gamma}_{X}^{-1}\mathcal{B})^{-1}\mathcal{B}^{'}\boldsymbol{\Gamma}_{X}^{-1}\boldsymbol{Y}$$

and $\hat{\boldsymbol{Y}} = \mathbf{H}\boldsymbol{Y}$, with $\mathbf{H} = \mathcal{B}(\mathcal{B}^{'}\boldsymbol{\Gamma}_{X}^{-1}\mathcal{B})^{-1}\mathcal{B}^{'}\boldsymbol{\Gamma}_{X}^{-1}$. The 95% confidence interval, using asymptotic normality, is $\hat{\boldsymbol{Y}} \pm 1.96\sqrt{\sigma_{X}^2 \mathrm{diag}\{\mathbf{H}\mathbf{H}'\}}$.

Estimation: penalized B-splines

The size of the basis determines the amount of smoothing of the fitted curves. The larger the value of J, the bumpier the fitting will be.

Eilers & Marx (1996) proposed the penalty

$$M^*_{\boldsymbol{\theta}} = ||\mathbf{T}\boldsymbol{Y} - \mathbf{T}\mathcal{B}\boldsymbol{\theta}||^2 + \lambda||\mathbf{D}_\ell\boldsymbol{\theta}||^2$$

λ is a positive regularization smoothing parameter
$\mathbf{D}_\ell$ constructs ℓ-th order differences of θ: $\mathbf{D}_\ell\boldsymbol{\theta} = \Delta^\ell\boldsymbol{\theta}$

$$\mathbf{D}_1 = \begin{pmatrix} -1 & 1 & 0 & 0 & \dots \\ 0 & -1 & 1 & 0 & \dots \\ 0 & 0 & -1 & 1 & \dots \\ \vdots & \vdots & \vdots & \vdots & \ddots \end{pmatrix} \text{ or } \mathbf{D}_2 = \begin{pmatrix} 1 & -2 & 1 & 0 & \dots \\ 0 & 1 & -2 & 1 & \dots \\ 0 & 0 & 1 & -2 & \dots \\ \vdots & \vdots & \vdots & \vdots & \ddots \end{pmatrix}$$

The penalized least square solution is

$$\hat{\boldsymbol{\theta}} = \sigma_X^2(\sigma_X^2\mathcal{B}'\boldsymbol{\Gamma}_X^{-1}\mathcal{B} + \lambda\mathbf{D}_\ell'\mathbf{D}_\ell)^{-1}\mathcal{B}'\boldsymbol{\Gamma}_X^{-1}\boldsymbol{Y}$$

and $\hat{\boldsymbol{Y}} = \mathbf{H}\boldsymbol{Y}$, with $\mathbf{H} = \sigma_X^2\mathcal{B}(\sigma_X^2\mathcal{B}'\boldsymbol{\Gamma}_X^{-1}\mathcal{B} + \lambda\mathbf{D}_\ell'\mathbf{D}_\ell)^{-1}\mathcal{B}'\boldsymbol{\Gamma}_X^{-1}$.

B-splines

A B-spline of degree d

- consists of $d+1$ polynomial pieces, each of degree d (=3);
- is connected by equidistant knots

Domain from x_{min} to x_{max} divided into m equal intervals by $m+1$ knots

- Each interval is covered by $d+1$ B-splines of degree d
- Number of B-splines is $n = m + d$

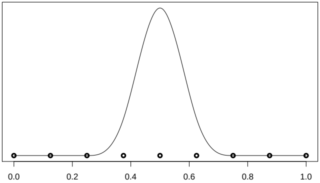

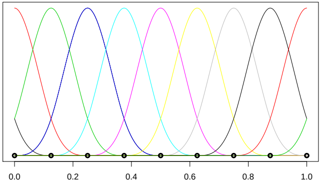

Simulation: Sinusoidal time-varying amplitudes

We simulate

$$Y_i = m(t_i) + \sum_{k=1}^{K} \{g_{1k}(t_i)\cos(w_k t_i) + g_{2k}(t_i)\sin(w_k t_i)\} + X_i, \qquad i = 1, \ldots, N,$$

with:

- Sample size $N = 500$
- Number of replication $M = 200$
- $K = 2$, $J = 29$, $d = 3$, $\lambda = 0.008$
- $m(t) = \sin(2\pi t)$
- $g_{11}(t) = \cos(9\pi t)$, $g_{21}(t) = \sin(15\pi t)$
- $g_{12}(t) = \cos(4\pi t)$, $g_{22}(t) = \sin(7\pi t)$
- $w_1 = 40\pi$, $w_2 = 100\pi$
- X_i, $i = 1, \ldots, N$ follows an AR(p) process, $p = 0, 1, 2$

$$X_t = \sum_{\ell=1}^{p} \phi_j X_{t-j} + Z_t, \qquad \{Z_t\} \overset{iid}{\sim} \mathcal{N}(0, 2)$$

Simulation: Polynomial time-varying amplitudes

We simulate

$$Y_i = m(t_i) + \sum_{k=1}^{K} \{g_{1k}(t_i)\cos(w_k t_i) + g_{2k}(t_i)\sin(w_k t_i)\} + X_i, \qquad i = 1, \ldots, N,$$

with:

- Sample size $N = 500$
- Number of replication $M = 200$
- $K = 2$, $J = 29$, $d = 3$, $\lambda = 0.008$
- $m(t) = 0.2t - 5t^2 + 5.5t^3$
- $g_{11}(t) = 4t^3 - 5t^5$, $g_{21}(t) = -0.5 - 0.5t + 2.5t^2 - 0.5t^3$
- $g_{12}(t) = -t + t^2 + 1.3t^3$, $g_{22}(t) = 0.5 + 2t^2 - 3t^3$
- $w_1 = 30\pi$, and $w_2 = 40\pi$.
- X_i, $i = 1, \ldots, N$ follows an AR(p) process, $p = 0, 1, 2$

$$X_t = \sum_{\ell=1}^{p} \phi_j X_{t-j} + Z_t, \qquad \{Z_t\} \overset{iid}{\sim} \mathcal{N}(0, 2)$$

Monte Carlo quantiles

confidence intervals for $\mu(t)$, $m(t)$, $g_{1k}(t)$ or $g_{2k}(t)$

For t fixed, using the normal distribution, and the sample mean and variance of $\boldsymbol{m}(t)$, $\boldsymbol{g}_{\ell k}(t)$, $l = 1, 2$, $k = 1, \dots, K$, and $\boldsymbol{\mu}(t)$, the confidence intervals are

$$\bar{m}(t) \pm 1.96 \sqrt{\frac{1}{M} \sum_{i=1}^{M} (\bar{m}(t) - \hat{m}^{(i)}(t))^2}$$

$$\bar{g}_{\ell k}(t) \pm 1.96 \sqrt{\frac{1}{M} \sum_{i=1}^{M} (\bar{g}_{\ell k}(t) - \hat{g}_{\ell k}^{(i)}(t))^2}, \qquad \ell = 1, 2, \qquad k = 1, \dots, K$$

$$\bar{\mu}(t) \pm 1.96 \sqrt{\frac{1}{M} \sum_{i=1}^{M} (\bar{\mu}_i(t) - \hat{\mu}^{(i)}(t))^2}$$

where $\bar{m}(t) = \frac{1}{M} \sum_{i=1}^{M} \hat{m}^{(i)}(t)$, $\bar{g}_{\ell k}(t) = \frac{1}{M} \sum_{i=1}^{M} \hat{g}_{\ell k}^{(i)}(t)$, $\ell = 1, 2$, $k = 1, \dots, K$, and $\bar{\mu}(t) = \frac{1}{M} \sum_{i=1}^{M} \hat{\mu}^{(i)}(t)$, $t = 1, \dots, N$.

Parametric quantiles

We know from the asymptotic properties of Least Squares that

$$\hat{\boldsymbol{\theta}} \sim \mathcal{N}(\sigma_X^2(\sigma_X^2\mathcal{B}^{'}\boldsymbol{\Gamma}_X^{-1}\mathcal{B}+\lambda\mathbf{D}_\ell^{'}\mathbf{D}_\ell)^{-1}\mathcal{B}^{'}\boldsymbol{\Gamma}_X^{-1}\mathcal{B}\boldsymbol{\theta},$$
$$\sigma_X^6(\sigma_X^2\mathcal{B}^{'}\boldsymbol{\Gamma}_X^{-1}\mathcal{B}+\lambda\mathbf{D}_d^{'}\mathbf{D}_\ell)^{-1}\mathcal{B}^{'}\boldsymbol{\Gamma}_X^{-1}(\boldsymbol{\Gamma}_X^{-1})'\mathcal{B}(\sigma_X^2\mathcal{B}^{'}\boldsymbol{\Gamma}_X^{-1}\mathcal{B}+\lambda\mathbf{D}_\ell^{'}\mathbf{D}_\ell)^{-1}).$$

Then, using the delta method, the distribution of $\hat{m}(t)$ is

$$\hat{m}(t) \sim \mathcal{N}(\sigma_X^2\mathfrak{B}(t)\mathbf{C}_m(\sigma_X^2\mathcal{B}^{'}\boldsymbol{\Gamma}_X\mathcal{B}+\lambda\mathbf{D}_\ell^{'}\mathbf{D}_\ell)^{-1}\mathcal{B}^{'}\boldsymbol{\Gamma}_X\mathcal{B}\boldsymbol{\theta},$$
$$\sigma_X^6\mathfrak{B}(t)\mathbf{C}_m(\sigma_X^2\mathcal{B}^{'}\boldsymbol{\Gamma}_X^{-1}\mathcal{B}+\lambda\mathbf{D}_d^{'}\mathbf{D}_\ell)^{-1}\mathcal{B}'\boldsymbol{\Gamma}_X^{-1}(\boldsymbol{\Gamma}_X^{-1})'\mathcal{B}(\sigma_X^2\mathcal{B}^{'}\boldsymbol{\Gamma}_X^{-1}\mathcal{B}+\lambda\mathbf{D}_\ell^{'}\mathbf{D}_\ell)^{-1}(\mathfrak{B}(t)\mathbf{C}_m)^{'}),$$

Finally, the confidence interval for $m(t)$ is

$$\mathfrak{B}(t)\mathbf{C}_m\hat{\boldsymbol{\theta}} \pm 1.96\sqrt{\sigma_X^6\mathfrak{B}(t)\mathbf{C}_m(\sigma_X^2\mathcal{B}'\boldsymbol{\Gamma}_X^{-1}\mathcal{B}+\lambda\mathbf{D}_\ell'\mathbf{D}_\ell)^{-1}\mathcal{B}'\boldsymbol{\Gamma}_X^{-1}(\boldsymbol{\Gamma}_X^{-1})'\mathcal{B}(\sigma_X^2\mathcal{B}'\boldsymbol{\Gamma}_X^{-1}\mathcal{B}+\lambda\mathbf{D}_\ell'\mathbf{D}_\ell)^{-1}(\mathfrak{B}(t)\mathbf{C}_m)'}.$$

For $g_{lk}(t)$, $l=1,2$, $k=1,\ldots,K$, we follow the same idea. The CI for $\mu(t)$ is

$$\mathcal{B}(t)\hat{\boldsymbol{\theta}} \pm 1.96\sqrt{\sigma_X^6\mathcal{B}(t)(\sigma_X^2\mathcal{B}'\boldsymbol{\Gamma}_X^{-1}\mathcal{B}+\lambda\mathbf{D}_\ell'\mathbf{D}_\ell)^{-1}\mathcal{B}'\boldsymbol{\Gamma}_X^{-1}(\boldsymbol{\Gamma}_X^{-1})'\mathcal{B}(\sigma_X^2\mathcal{B}'\boldsymbol{\Gamma}_X^{-1}\mathcal{B}+\lambda\mathbf{D}_\ell'\mathbf{D}_\ell)^{-1}\mathcal{B}(t)'}.$$

Simulation: Sinusoidal vs Polynomial t-v parameters

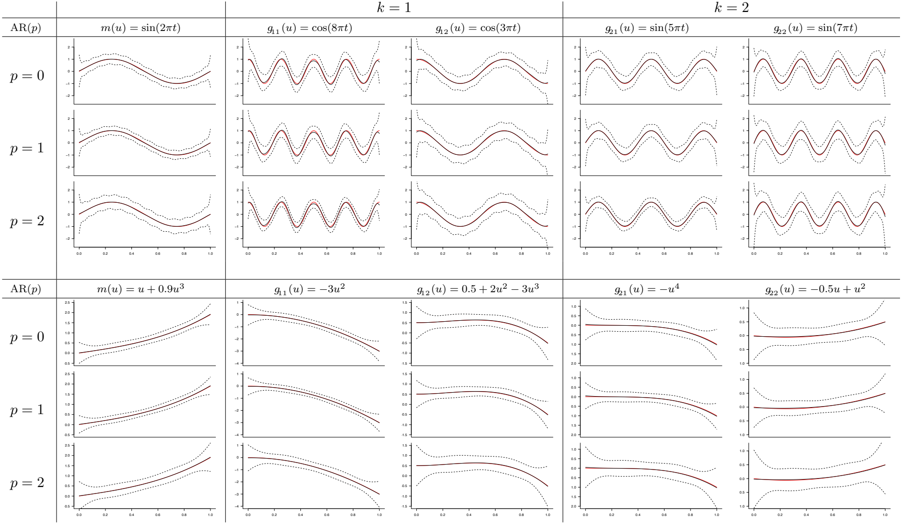

Simulation: Sinusoidal parameters

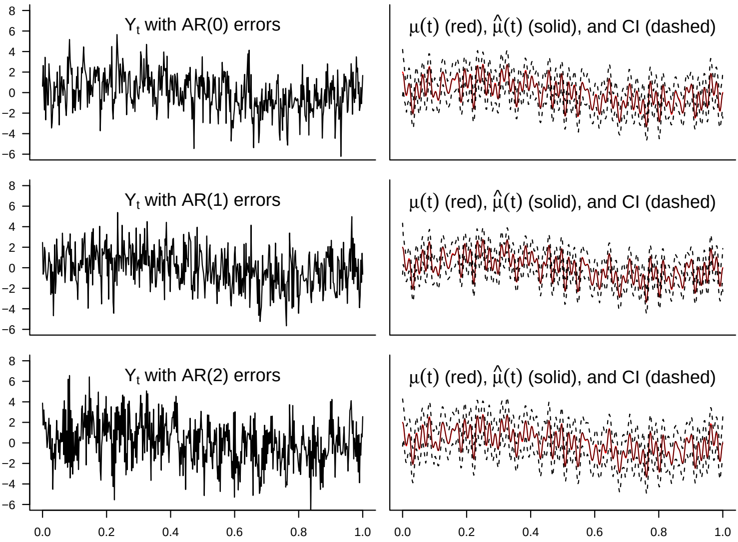

Simulation: Polynomial parameters

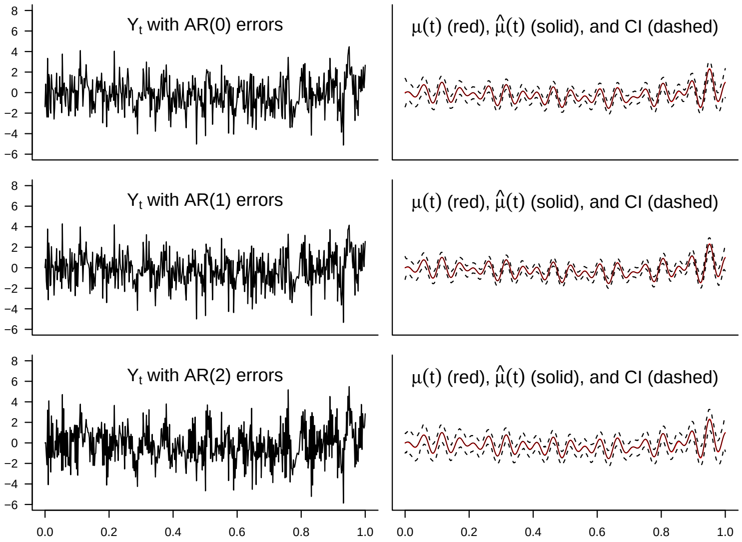

Simulated RR Lyrae ("realistic parameters")

Amplitude modulated RR Lyrae light curve

We simulate the data according to Benko et al. (2011) as

$$Y_t = \left[1 + \frac{U_m(t)}{U_c}\right]\left[a_0 + \sum_{k=1}^{10} a_k \sin(2\pi k f_0 t + \varphi_k)\right] + X_t$$

where

- $c(t) = a_0 + \sum_{k=1}^{10} a_k \sin(2\pi k f_0 t + \varphi_k)$ is the carrier wave with ten harmonics
- $U_m(t) = a_m \sin(2\pi f_m t + \varphi_m)$ is the modulation signal
- U_c is the amplitude of the non-modulated light curve
- $X_t \overset{iid}{\sim} \mathcal{N}(0, 0.0625)$, with $\boldsymbol{t}$ between 0 and 10.4 days.

Simulated RR Lyrae ("realistic parameters")

Benko et al. (2011)

Frequency day^{-1}	Amplitude mag	Phase $rad/2\pi$	Identification
2	0.40152	5.49	f_0
4	0.17093	144.04	$2f_0$
6	0.13256	285.25	$3f_0$
8	0.09676	81.29	$4f_0$
10	0.07044	239.35	$5f_0$
12	0.04642	37.62	$6f_0$
14	0.03049	200.01	$7f_0$
16	0.01850	353.29	$8f_0$
18	0.01073	151.69	$9f_0$
20	0.00619	312.09	$10f_0$

Table: Frequencies, amplitudes, phases parameters, $a_0 = 0.01$, $f_m = 0.05\ day^{-1}$, and $\varphi_m = 4.712388\ rad/2\pi$ obtained from Benko et al. (2011).

Simulated RR Lyrae ("realistic parameters")

Benko et al. (2011)

We can rewrite the model as

$$Y_t = \mu(t) + \varepsilon_t,$$

with

$$\mu(t) = m(t) + \sum_{k=1}^{10} g_{2k}(t) \sin(2\pi k f_0 t + \varphi_k),$$

where

$$m(t) = a_0(1 + U_m(t)/U_c), \quad g_{2k}(t) = a_k[1 + U_m(t)/U_c], \quad k = 1, ..., 10.$$

Simulated RR Lyrae ("realistic parameters")

Benko et al. (2011)

We fit the model

$$Y_t = m(t) + \sum_{k=1}^{10} g_{2k}(t)\sin(2\pi k f_0 t + \varphi_k) + X_t.$$

where:
- $m(t) = \sum_{j=1}^{J} \alpha_j B_j(t)$
- $g_{2k}(t) = \sum_{j=1}^{J} \gamma_{kj} B_j(t)$, $k = 1, \ldots, 10$

We assume that we know the frequency f_0, and the phase φ_k, $k = 1, \ldots, 10$.

Parameters λ, the number of B-spline in the basis J, and the order d are 0.001, 4, and 3, respectively.

Simulated RR Lyrae ("realistic parameters")

Benko et al. (2011)

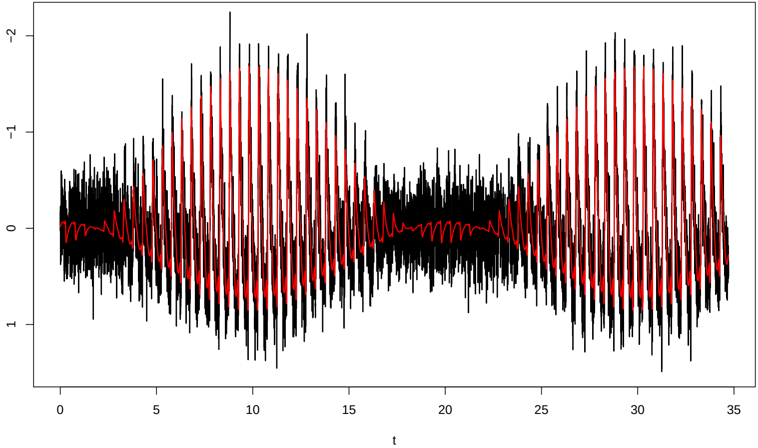

Simulated RR Lyrae ("realistic parameters")

Benko et al. (2011)

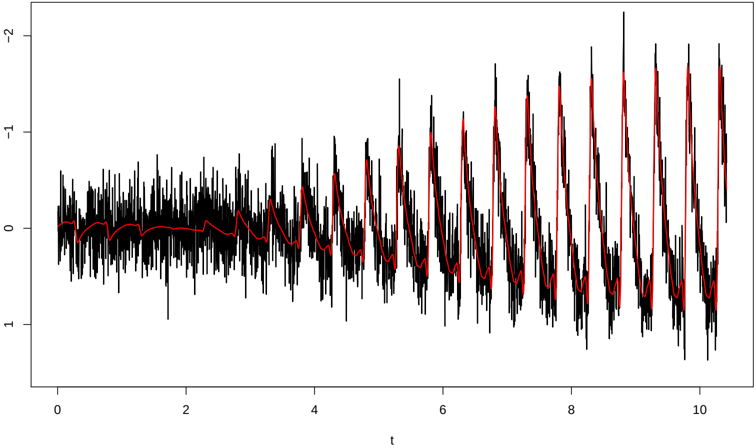

Estimated RR Lyrae ("realistic parameters")

Benko et al. (2011)

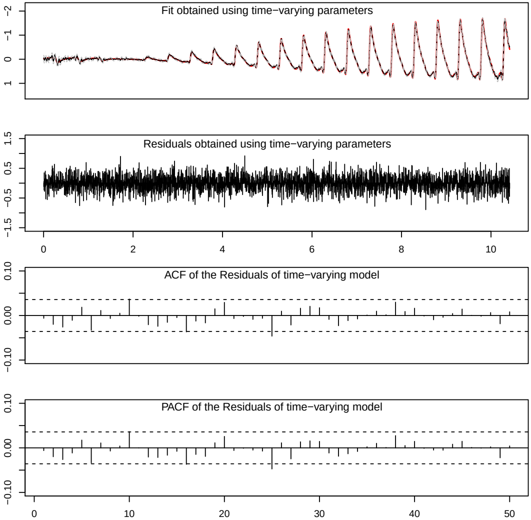

Estimated RR Lyrae (“realistic parameters”)

Benko et al. (2011)

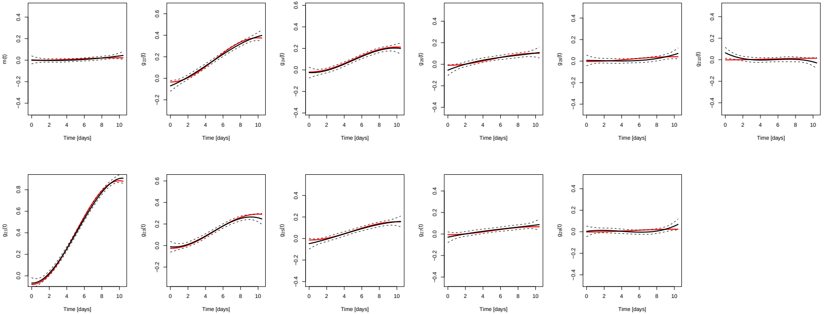

Outline

RR Lyrae CSS J234345.7+015205

- Belonging to the Pisces constellation, observed with the Kepler space telescope over the 8.9-day long K2 Two-Wheel Concept Engineering Test.
- The data is available online from the Konkoly Observatory of the Hungarian Academy of Sciences webpage[1].
- Benkő et el. (2011) mentioned that RR Lyrae stars show change pulsation amplitudes: this star is modulated.

Molnar et al. (2015) fitted the following model

$$Y_i = m + \sum_k A_k \sin(2\pi[k f_0 t + \phi_k]) + X_i. \tag{16}$$

- To estimate the main pulsation frequencies f_0, the harmonics $k f_0$, the amplitudes A_k and the phases ϕ_k, $k = 1, 2, ..., K$, they used `Period04` software.
- To fit model (16), `Period04` applies the Levenberg-Marquardt non-linear least-squares fitting procedure. With this software, they detected 10 significant harmonics which are shown in Table 2.

---

[1] https : //konkoly.hu/KIK/data_en.html

RR Lyrae CSS J234345.7+015205

Frequency day^{-1}	Amplitude mag	Phase $rad/2\pi$	Identification
1.612	0.2452	0.441	f_0
3.223	0.1154	0.255	$2f_0$
4.836	0.0834	0.105	$3f_0$
6.447	0.0539	0.971	$4f_0$
8.059	0.0369	0.843	$5f_0$
9.671	0.0214	0.728	$6f_0$
11.283	0.0109	0.591	$7f_0$
12.895	0.0076	0.426	$8f_0$
14.507	0.0044	0.312	$9f_0$
16.119	0.0033	0.283	$10f_0$

Table: Frecuency table of RR Lyrae star in EPIC 60018778 data set: frequencies, amplitudes, phases, and the identification of the peaks (f_0: main pulsation frequency) from Molnar et al. (2015)

RR Lyrae CSS J234345.7+015205

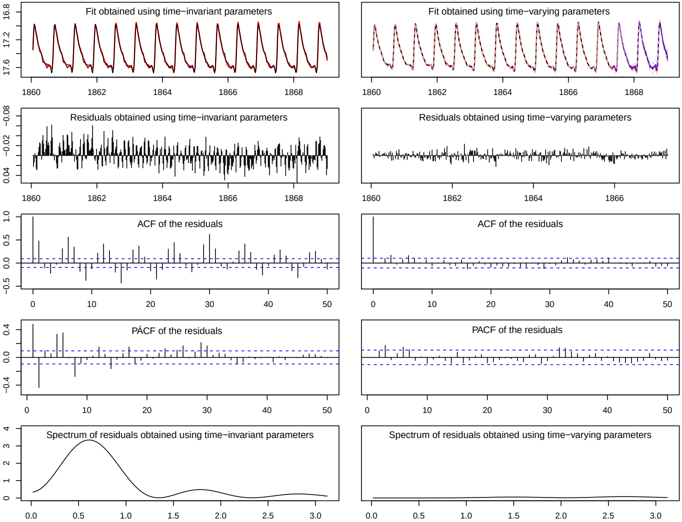

Periodogram for unequally spaced data

Deeeming (1974) found the relation

$$\mathbb{E}[F_N(v)F_N^*(v)] = \sigma^2 P(v) * V_N(v),$$

where

$F_N(v) = \sum_{j=1}^{N} X(t_j)\exp(i\lambda_v t_j), \quad \lambda_v = 2\pi v, \quad$ is the discrete Fourier transform,
$P(v) = \int_{-\infty}^{\infty} \gamma(r)\exp(i\lambda_v r)dr$ is the power spectrum,
$\gamma(r)$ is the autocorrelation function of the stationary stochastic process $X(t_j)$,
$V_N(v) = \sum_{j,k} \exp(i\lambda_v(t_j - t_k))$,
$F_N^*(v)$ is the conjugate of $F_N(v)$,
$P(v) * V_N(v)$ is the convolution of the power spetrum $P(v)$ with $V_N(v)$
σ^2 is variance of the stationary stochastic process $X(t_j)$

If $X(t_j)$, $j = 1, \ldots, N$ is iid $\mathcal{N}(0, \sigma^2)$ then

$$\mathbb{E}[F_N(v)F_N^*(v)] = N\sigma^2$$

Outline

Non-stationary CARMA(5,3) model

from Kelly et al. (2014)

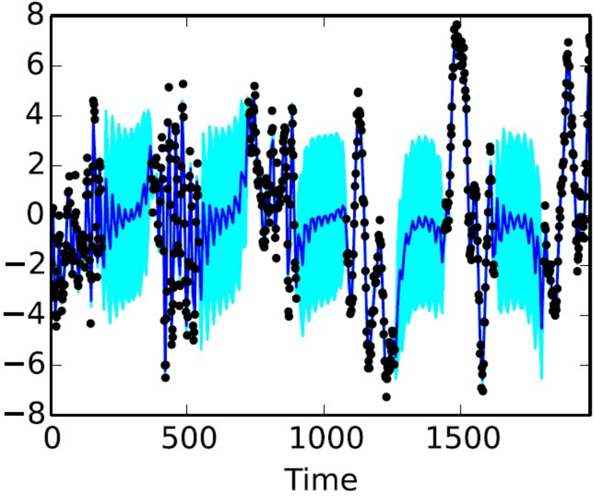

Non-stationarity: the parameters change from the first to the second half.

OGLE-LMC-LPV-00005

from Kelly et al. (2014)

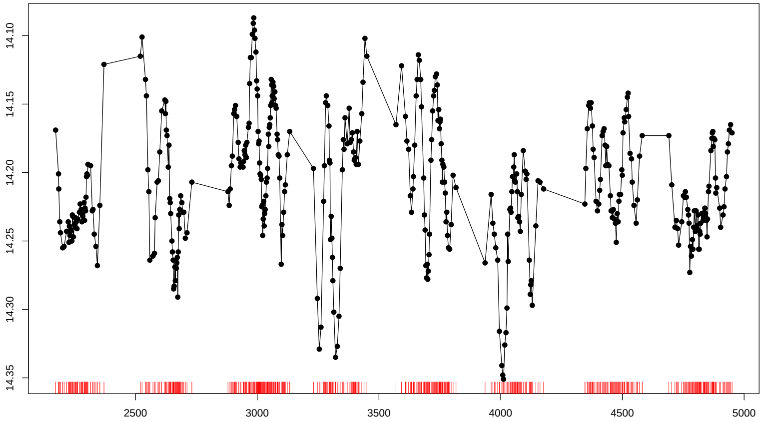

Data obtained from `https://github.com/brandonckelly/carma_pack`.

OGLE-LMC-LPV-00005

from Kelly et al. (2014)

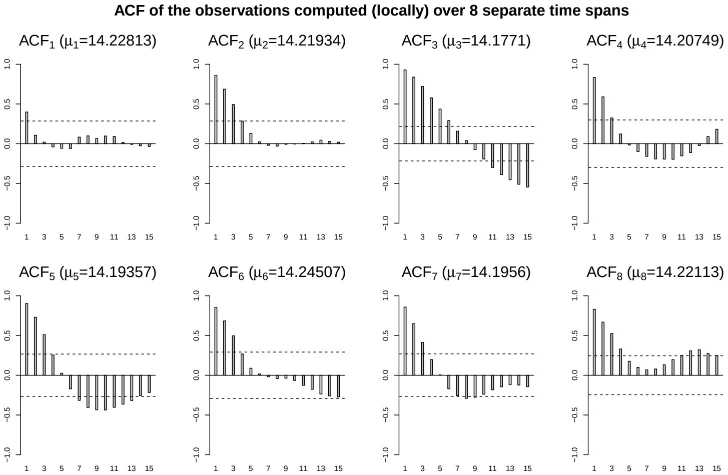

OGLE-LMC-LPV-00005

from Kelly et al. (2014)

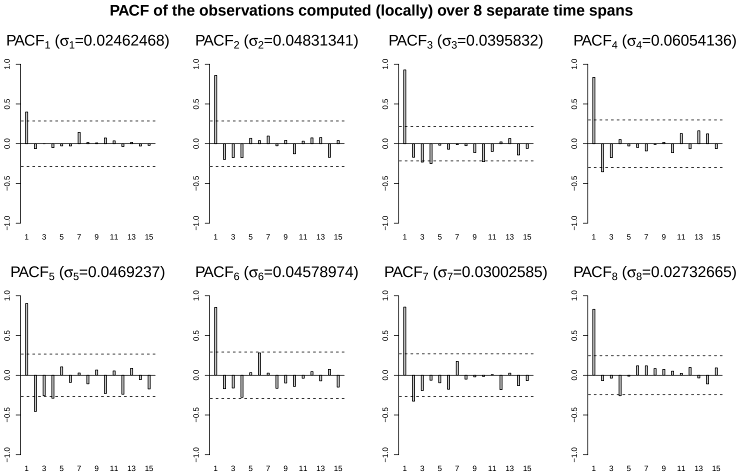

Outline

CARMA(p, q) process

A p, q order continuous time autoregressive moving average (CARMA(p, q)) process $y(t)$ is defined to be the solution of

$$\frac{d^p y(t)}{dt^p} + \alpha_{p-1} \frac{d^{p-1} y(t)}{dt^{p-1}} + ... + \alpha_0 y(t) = \beta_q \frac{d^q \varepsilon(t)}{dt^q} + \beta_{q-1} \frac{d^{q-1} \varepsilon(t)}{dt^{q-1}} + ... + \varepsilon(t)$$

where:

$\varepsilon(t)$ continuous time white noise process with zero mean and variance σ^2

Time-invariant parameters $\alpha_0, ..., \alpha_{p-1}$ are the autoregressive coefficients

Time-invariant Parameters $\beta_0, ..., \beta_q$ are the moving average coefficients

Stationary condition

1) $q < p$
2) The roots $r_1, ..., r_p$ of the autoregressive polynomial $A(z) = \sum_{k=0}^{p} \alpha_k z^k$ have negative real parts

Non-stationarity

Non-stationarity: Astronomy

Accretion physics

Phenomenological model of the PSD: a sum of Lorenzian functions
Belloni, Psaltis, van der Klis 2002

All frequencies increase together, and each component is strongly suppressed as it approaches ~5 Hz,

Done, Gierlinski & Kubota 2006
(after Axelsson et al. 2005; Cyg X-1)

CENTER FOR ASTROPHYSICS
HARVARD & SMITHSONIAN

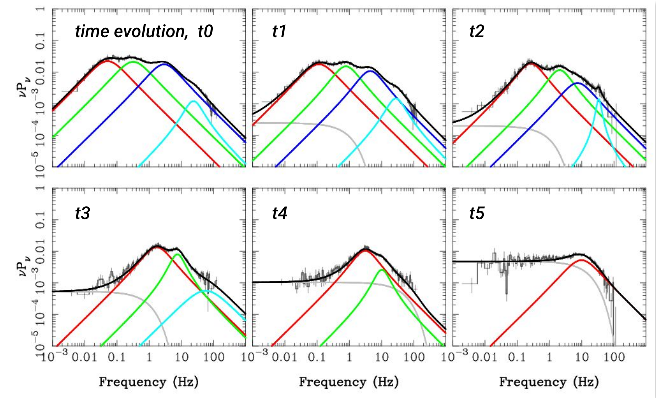

e.g. propagation of random mass accretion rate fluctuations through the accretion disk toward its inner edge

Non-stationarity: Astronomy

CARMA. Modeling astronomical time series in the time domain

Autocovariance function at lag τ

$$A(z) = \sum_{k=0}^{p} \alpha_k z^k$$

$$R(\tau) = \sigma^2 \boxed{\sum_{k=1}^{p}} \frac{\left[\sum_{l=0}^{q} \beta_l r_k^l\right]\left[\sum_{l=0}^{q} \beta_l (-r_k)^l\right] \boxed{\exp(r_k \tau)}}{-2\,\mathrm{Re}(r_k) \prod_{l=1, l \neq k}^{p} (r_l - r_k)(r_l^* + r_k)}$$

Number of Lorenzians?

Order p of the AR polynomial
+
Roots come in complex conjugate pairs

- weighted sum of ***p*** exponential functions
- **weights** are functions of **MA coefficients,** β
- **arguments** depend on the **roots of AR polynomial** that might be complex-valued
  - exponentially damped sinusoids for complex roots,
  - exponential decays for real roots.
- PSD and autocovariance are a Fourier pair, so **PSD of a CARMA process** can be expressed as a weighted **sum of Lorentzian functions**, with centroids ~ |Im(roots)| and widths ~ |Re(roots)|

see e.g. Nowak 2000, Belloni 2010, McHardy 2007
for observed X-ray PSDs of X-ray binaries and AGN

CENTER FOR ASTROPHYSICS
HARVARD & SMITHSONIAN

Non-stationarity: Astronomy

Alston et al. (2018)

- The light curves exhibit significant strong non-stationarity, in addition to that caused by the rms-flux relation, and are fractionally more variable at lower source flux.
- The non-stationarity is manifest in the PSD with the normalisation of the peaked components increasing with decreasing source flux, as well as the low-frequency peak moving to higher frequencies.
- The Authors discuss the implication of these results for accretion of matter onto black holes.

Alston (2019)

- investigates the effects of *piecewise* non-stationary power spectra on the resultant flux distribution and rms-flux relation.

Non-stationarity: Statistics

Csőrgő and Horváth (1997)

- H_0: structural stability, $H_1 : \exists$ one or multiple structural break(s).
- If H_0 is rejected, the locations of the breaks need to be estimated

Non-stationarity: Statistics

Structural breaks

Csőrgő and Horváth (1997)

- H_0: structural stability, $H_1 : \exists$ one or multiple structural break(s).
- If H_0 is rejected, the locations of the breaks need to be estimated

Horváth et al. (1999): $\boxed{X(t) = \mu_t + \varepsilon(t)}$

$$H_0 \quad \mu_1 = \mu_2 = \cdots = \mu_T \equiv \mu$$

$$H_A^{(1)} \quad \mu_1 = \mu_2 = \mu_{k^*} \neq \mu_{k^*+1} = \cdots = \mu_T$$

$$H_A^{(2)} \quad H_1 : \mu_1 = \mu_2 = \mu_{k^*} \neq \mu_{j^*+1} = \cdots = \mu_T$$

$$\mu_{k^*+t} = \mu_{k^*} - \frac{\mu_{k^*} - \mu_T}{j^* - k^*} t, \quad 1 \leq t \leq j^* - k^*$$

Non-stationarity: Statistics

Structural breaks

Csőrgő and Horváth (1997)

- H_0: structural stability, $H_1 : \exists$ one or multiple structural break(s).
- If H_0 is rejected, the locations of the breaks need to be estimated

Horváth et al. (1999): $\boxed{X(t) = \mu_t + \varepsilon(t)}$

H_0 $\mu_1 = \mu_2 = \cdots = \mu_T \equiv \mu$

$H_A^{(1)}$ $\mu_1 = \mu_2 = \mu_{k^*} \neq \mu_{k^*+1} = \cdots = \mu_T$

$H_A^{(2)}$ $H_1 : \mu_1 = \mu_2 = \mu_{k^*} \neq \mu_{j^*+1} = \cdots = \mu_T$

$\mu_{k^*+t} = \mu_{k^*} - \frac{\mu_{k^*} - \mu_T}{j^* - k^*} t, \;\; 1 \leq t \leq j^* - k^*$

Aue and Horváth (2011): $\boxed{X(t) = \alpha_t X(t-1) + \varepsilon(t)}$,

H_0 $\alpha_1 = \alpha_2 = \cdots = \alpha_T \equiv \alpha$

H_1 $\alpha_1 = \alpha_2 = \alpha_{k^*} \neq \alpha_{k^*+1} = \cdots = \alpha_T$

Non-stationarity: Statistics

Structural breaks

Aue and Horváth (2011): $X(t) = \alpha_t X(t-1) + \varepsilon(t)$

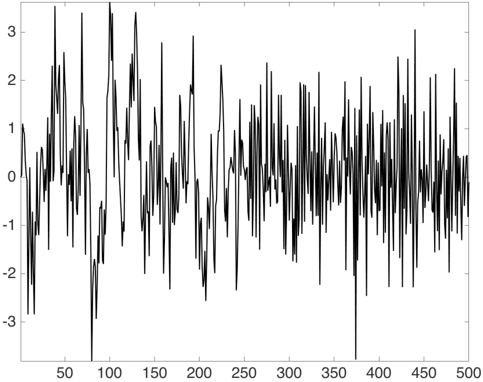

Non-stationarity: Statistics

Structural breaks

Aue and Horváth (2011): $X(t) = \begin{cases} 0.6X(t-1) + \varepsilon(t) & 1 \leq t \leq 250 \\ -0.2X(t-1) + \varepsilon(t) & 250 < t \leq 500 \end{cases}$

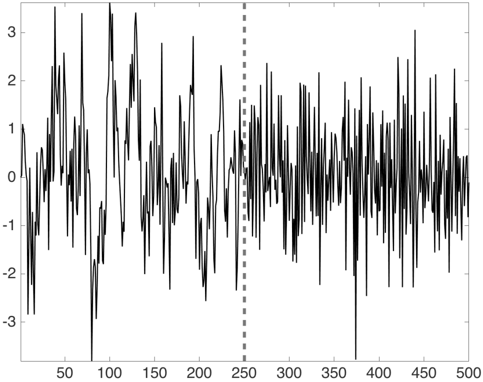

Non-stationarity: Statistics

Structural breaks

$$\mathrm{Var}[X(t)] = \frac{\sigma_\varepsilon^2}{1-\alpha_t^2}$$

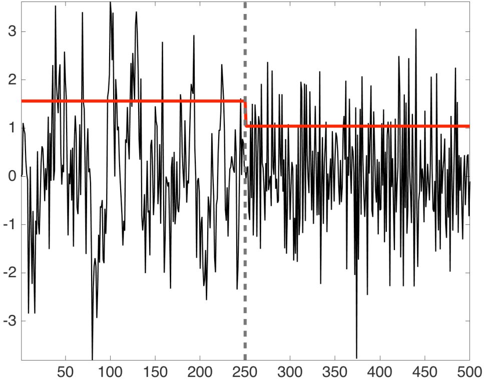

Non-stationarity: Statistics

Locally stationary process: Dahlhaus (1997, 2000)

Locally stationary ARMA (LSARMA(p, q)) process: the solution of

$$y_{i,N} = \sum_{j=1}^{p} \alpha_j \left(\frac{t_i}{t_N}\right) y_{i-j,N} + \varepsilon_{i,N} + \sum_{j=1}^{q} \beta_j \left(\frac{t_i}{t_N}\right) \varepsilon_{i-j,N}, \quad i = 1, ..., N$$

where $\varepsilon(t) \sim WN(0, \sigma^2)$ and

$\alpha_1(u), ..., \alpha_p(u)$: time-varying AR coefficients
$\beta_1(u), ..., \beta_q(u)$: time-varying MA coefficients

A simulated Locally Stationary AR(2)

$$X_{t+1} = \alpha_1(\tfrac{t}{T})X_t + \alpha_2(\tfrac{t}{T})X_{t-1} + \sigma_\varepsilon(\tfrac{t}{T})\varepsilon_{t+1}$$

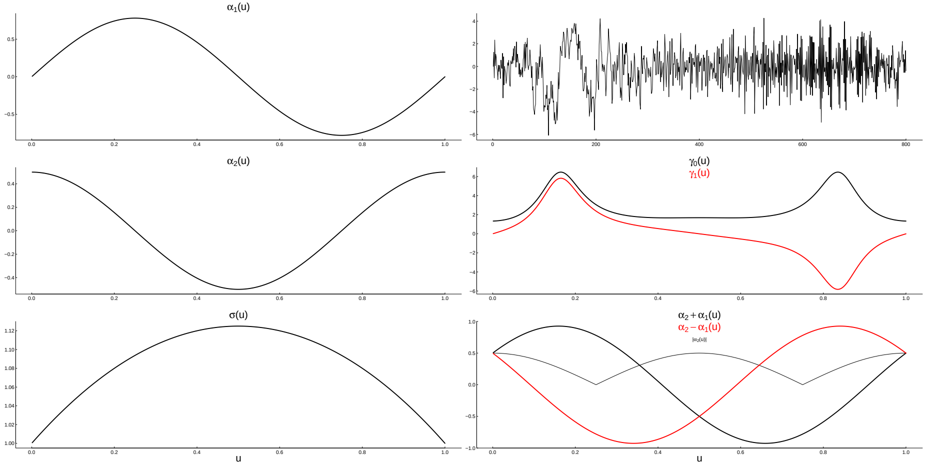

Localized Yule-Walker: $p = 2$

$$
\begin{array}{rcccccc}
X_{s+1} & = & \alpha_1(\frac{s}{T})X_s & + & \alpha_2(\frac{s}{T})X_{s-1} & + & \sigma_\varepsilon(\frac{s}{T})\varepsilon_{s+1} \\
X_{s+1} & = & \alpha_1(\frac{s}{T})X_s & + & \alpha_2(\frac{s}{T})X_{s-1} & + & \sigma_\varepsilon(\frac{s}{T})\varepsilon_{s+1} \\
X_{s+1} & = & \alpha_1(\frac{s}{T})X_s & + & \alpha_2(\frac{s}{T})X_{s-1} & + & \sigma_\varepsilon(\frac{s}{T})\varepsilon_{s+1}
\end{array}
$$

Localized Yule-Walker: $p = 2$

$$\begin{pmatrix} X_{s+1} & 0 & 0 \\ 0 & X_s & 0 \\ 0 & 0 & X_{s-1} \end{pmatrix} \qquad \begin{array}{rcrcrcr} X_{s+1} & = & \alpha_1(\frac{s}{T})X_s & + & \alpha_2(\frac{s}{T})X_{s-1} & + & \sigma_\varepsilon(\frac{s}{T})\varepsilon_{s+1} \\ X_{s+1} & = & \alpha_1(\frac{s}{T})X_s & + & \alpha_2(\frac{s}{T})X_{s-1} & + & \sigma_\varepsilon(\frac{s}{T})\varepsilon_{s+1} \\ X_{s+1} & = & \alpha_1(\frac{s}{T})X_s & + & \alpha_2(\frac{s}{T})X_{s-1} & + & \sigma_\varepsilon(\frac{s}{T})\varepsilon_{s+1} \end{array}$$

$$\begin{array}{rcccccc} X_{s+1}^2 & = & \alpha_1(\frac{s}{T})X_{s+1}X_s & + & \alpha_2(\frac{s}{T})X_{s+1}X_{s-1} & + & \sigma_\varepsilon(\frac{s}{T})X_{s+1}\varepsilon_{s+1} \\ X_sX_{s+1} & = & \alpha_1(\frac{s}{T})X_s^2 & + & \alpha_2(\frac{s}{T})X_sX_{s-1} & + & \sigma_\varepsilon(\frac{s}{T})X_s\varepsilon_{s+1} \\ X_{s-1}X_{s+1} & = & \alpha_1(\frac{s}{T})X_{s-1}X_s & + & \alpha_2(\frac{s}{T})X_{s-1}^2 & + & \sigma_\varepsilon(\frac{s}{T})X_{s-1}\varepsilon_{s+1} \end{array}$$

Localized Yule-Walker: $p = 2$

Use 5 observations $X_{t\pm 2}$, local stationarity at fixed $u \in [\frac{t-1}{T}, \frac{t+1}{T}[$

$$\alpha_2(\tfrac{t\pm 1}{T}) \approx \alpha_2(u), \qquad \alpha_1(\tfrac{t\pm 1}{T}) \approx \alpha_1(u), \qquad \sigma_\varepsilon^2(\tfrac{t\pm 1}{T}) \approx \sigma_\varepsilon^2(u),$$

and $\mathbb{E}[X_s \varepsilon_t] = 0$ whenever $s < t$

$$\begin{aligned}
\sum_{s=t-1}^{t+1} X_{s+1}^2 &\approx \alpha_1(u) \sum_{s=t-1}^{t+1} X_{s+1} X_s + \alpha_2(u) \sum_{s=t-1}^{t+1} X_{s+1} X_{s-1} + \sigma_\varepsilon^2(u) \\
\sum_{s=t-1}^{t+1} X_s X_{s+1} &\approx \alpha_1(u) \sum_{s=t-1}^{t+1} X_s^2 + \alpha_2(u) \sum_{s=t-1}^{t+1} X_s X_{s-1} \\
\sum_{s=t-1}^{t+1} X_{s-1} X_{s+1} &\approx \alpha_1(u) \sum_{s=t-1}^{t+1} X_{s-1} X_s + \alpha_2(u) \sum_{s=t-1}^{t+1} X_{s-1}^2
\end{aligned}$$

Localized Yule-Walker: $p = 2$

First smooth $\mathbf{G}_K^{yw}(u_t; K)$, then invert $\overline{\mathbf{\Gamma}}_K^{yw}(u; h, K)$:

Localized Yule-Walker: $p = 2$

First smooth $\mathbf{G}_K^{yw}(u_t; K)$, then invert $\overline{\mathbf{\Gamma}}_K^{yw}(u; h, K)$:

$$\overline{\mathbf{\Gamma}}_K^{yw}(u; h, K) = \sum_{t=2}^{T-1} \omega_t(u; h) \mathbf{G}_K^{yw}(u_t; K) = \sum_{t=2}^{T-1} \omega_t(u; h) \begin{pmatrix} X_t^2 & X_{t-1} X_t \\ X_{t-1} X_t & X_{t-1}^2 \end{pmatrix}$$

$$\begin{bmatrix} \bar{\mathrm{a}}_1(u; h) \\ \bar{\mathrm{a}}_2(u; h) \end{bmatrix} := \left[\sum_{t=2}^{T-1} \omega_t(u; h) \begin{pmatrix} X_t^2 & X_{t-1} X_t \\ X_{t-1} X_t & X_{t-1}^2 \end{pmatrix} \right]^{-1} \left[\sum_{t=2}^{T-1} \omega_t(u; h) \begin{pmatrix} X_t X_{t+1} \\ X_{t-1} X_{t+1} \end{pmatrix} \right]$$

$$\mathrm{s}_\varepsilon^2(u_t) := \sum_{t=2}^{T-1} \omega_t(u; h) X_{t+1}^2 - [\bar{\mathrm{a}}_1(u; h),\ \bar{\mathrm{a}}_2(u; h)] \left[\sum_{t=2}^{T-1} \omega_t(u; h) \begin{pmatrix} X_t X_{t+1} \\ X_{t-1} X_{t+1} \end{pmatrix} \right]$$

Target: $\Gamma_K(u)$

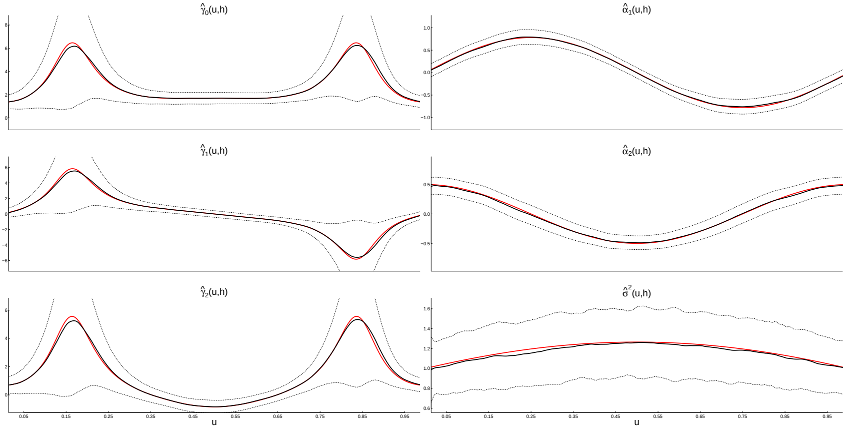

Outline

Estimation of the LSAR(p) process

Model

$$y_{i,N} = \sum_{j=1}^{p} \alpha_j\left(\frac{t_i}{t_N}\right) y_{i-j,N} + \varepsilon_{i,N} \tag{17}$$

Assumption

$$\alpha_j\left(\frac{t_i}{t_N}\right) = \sum_{l=1}^{L} a_{jl} B_{jl}\left(\frac{t_i}{t_N}\right)$$

Vector of coefficient $\boldsymbol{\gamma}^* = (a_{11}, ..., a_{1L}, a_{21}, ..., a_{2L}, ..., a_{p1}, ..., a_{pL})'$ is estimated by least squares linear regression

Minimizing with respect to $\boldsymbol{\gamma}^*$

$$S(\boldsymbol{\gamma}^*) = \sum_{t=m+1+q}^{N} \left\{ y_{i,N} - \left(\sum_{l=1}^{L} a_{1l} B_l\left(\frac{t_i}{t_N}\right)\right) y_{i-1,N} - \ldots - \left(\sum_{l=1}^{L} a_{pl} B_l\left(\frac{t_i}{t_N}\right)\right) y_{i-p,N} \right\}^2$$

Estimation of the LSAR(p) process

Solution

$$\widehat{\gamma^*} = (\mathbf{Z}'\mathbf{Z})^{-1}\mathbf{Z}\boldsymbol{y}_{N},$$

where $\boldsymbol{y}_N = (y_{p+1}, ..., y_N)'$ and $\mathbf{Z}$ is the $(N-p) \times Lp$ matrix

$$\mathbf{Z} = \begin{pmatrix}
B_1\left(\frac{t_{p+1}}{t_N}\right) y_{p,N} & \cdots & B_L\left(\frac{t_{p+1,N}}{t_N}\right) y_{p,N} & \cdots & B_L\left(\frac{t_{p+1,N}}{t_N}\right) y_{1,N} & \cdots & B_L\left(\frac{t_{p+1}}{t_N}\right) y_{1,N} \\
B_1\left(\frac{t_{p+2}}{t_N}\right) y_{p+1,N} & \cdots & B_L\left(\frac{t_{p+2}}{t_N}\right) y_{p+1,N} & \cdots & B_L\left(\frac{t_{p+2}}{t_N}\right) y_{2,N} & \cdots & B_L\left(\frac{t_{p+2}}{t_N}\right) y_{2,N} \\
\vdots & \vdots & \vdots & \vdots & \vdots & \vdots & \vdots \\
B_1\left(\frac{t_N}{t_N}\right) y_{N-1,N} & \cdots & B_L\left(\frac{t_N}{t_N}\right) y_{N-1,N} & \cdots & B_L\left(\frac{t_N}{t_N}\right) y_{N-p,N} & \cdots & B_L\left(\frac{t_N}{t_N}\right) y_{N-p,N}
\end{pmatrix}$$

Estimation of the LSAR(p) process

Number of coefficients in the model (17)

$p = 1 \Rightarrow L$ coefficients

$p = 2 \Rightarrow 2L$ coefficients

...

$p \Rightarrow pL$ coefficients

If L is large: **Penalization**

Minimizing

$$S(\boldsymbol{\gamma}^*) = \|\boldsymbol{y}_N - \mathbf{Z}\boldsymbol{\gamma}^*\|^2 + \lambda \|\mathbf{D}_\ell \boldsymbol{\gamma}^*\|^2$$

λ: positive regularization smoothing parameter $\mathbf{D}_\ell \boldsymbol{\gamma}^*$: $\Delta^\ell \boldsymbol{\gamma}^*$

Solution

$$\widehat{\boldsymbol{\gamma}^*} = (\mathbf{Z}'\mathbf{Z} + \lambda \mathbf{D}_\ell' \mathbf{D}_\ell)^{-1} \mathbf{Z} \boldsymbol{y}_N,$$

Estimation of the LSARMA(p,q) process

Hannan-Rissanen estimation procedure with B-splines

$$y_{i,N} = \sum_{j=1}^{p} \alpha_j \left(\frac{t_i}{t_N}\right) y_{i-j,N} + \varepsilon_{i,N} + \sum_{j=1}^{q} \beta_j \left(\frac{t_i}{t_N}\right) \varepsilon_{i-j,N}, \quad i = 1, ..., N$$

Step 1.

A high-order LSAR(m) model $(m > \max(p,q))$ is fitted using the methodology mentioned before (for LSAR(p))

Then the estimated residuals are computed from the equation

$$\widehat{\varepsilon}_{i,N} = y_{i,N} - \widehat{\alpha}_{m1} \left(\frac{t_i}{t_N}\right) y_{i-1,N} - ... - \widehat{\alpha}_{mm} \left(\frac{t_i}{t_N}\right) y_{i-m,N}, \quad i = m+1, ..., N$$

Step 2.

$$\text{Assumption: } \alpha_j \left(\frac{t_i}{t_N}\right) = \sum_{l=1}^{L} a_{jl} B_l \left(\frac{t_i}{t_N}\right), \qquad \beta_j \left(\frac{t_i}{t_N}\right) = \sum_{l=1}^{L} b_{jl} B_l \left(\frac{t_i}{t_N}\right).$$

Then we estimate by OLS the vector of parameters

$\boldsymbol{\gamma}^* = (a_{11}, ..., a_{1L}, a_{21}, ..., a_{2L}, ..., a_{p1}, ..., a_{pL}, b_{11}, ..., b_{1L}, b_{21}, ..., b_{2L}, ..., b_{q1}, ..., b_{qL})'$

Estimation of the LSARMA(p, q) process

Minimizing

$$S(\boldsymbol{\gamma}^*) = \sum_{t=m+1+q}^{N} \{ y_{i,N} - \left(\sum_{l=1}^{L} a_{1l} B_l \left(\frac{t_i}{t_N} \right) \right) y_{i-1,N} - \dots - \left(\sum_{l=1}^{L} a_{pl} B_l \left(\frac{t_i}{t_N} \right) \right) y_{i-p,N}$$
$$- \left(\sum_{l=1}^{L} b_{1l} B_l \left(\frac{t_i}{t_N} \right) \right) \widehat{\epsilon}_{i-1,N} - \dots - \left(\sum_{l=1}^{L} b_{ql} B_l \left(\frac{t_i}{t_N} \right) \right) \widehat{\epsilon}_{i-q,N} \}^2$$

Solution

$$\widehat{\boldsymbol{\gamma}}^* = (\mathbf{Z}'\mathbf{Z})^{-1} \mathbf{Z} \boldsymbol{y}_N \,,$$

where $\boldsymbol{y}_N = (y_{m+1+q}, \dots, y_N)'$ and $\mathbf{Z}$ is the $(N - m - q) \times L(p + q)$ matrix

$$\mathbf{Z} = \left(\begin{matrix} B_1\left(\frac{t_{m+1+q}}{t_N}\right) y_{m+q} & \cdots & B_L\left(\frac{t_{m+1+q}}{t_N}\right) y_{m+q} & \cdots & B_1\left(\frac{t_{m+1+q}}{t_N}\right) y_{m+q+1-p} & \cdots & B_L\left(\frac{t_{m+1+q}}{t_N}\right) y_{m+q+1-} \\ B_1\left(\frac{t_{m+2+q}}{t_N}\right) y_{m+q+1} & \cdots & B_L\left(\frac{t_{m+2+q}}{t_N}\right) y_{m+q+1} & \cdots & B_1\left(\frac{t_{m+2+q}}{t_N}\right) y_{m+q+2-p} & \cdots & B_L\left(\frac{t_{m+2+q}}{t_N}\right) y_{m+q+2-} \\ \vdots & \ddots & \vdots & \ddots & \vdots & \ddots & \vdots \\ B_1\left(\frac{t_N}{t_N}\right) y_{N-1} & & B_L\left(\frac{t_N}{t_N}\right) y_{N-1} & & B_1\left(\frac{t_N}{t_N}\right) y_{N-p} & & B_L\left(\frac{t_N}{t_N}\right) y_{N-p} \end{matrix} \right.$$

$$\left. \begin{matrix} B_1\left(\frac{t_{m+1+q}}{t_N}\right) \widehat{\epsilon}_{m+q} & \cdots & B_L\left(\frac{t_{m+1+q}}{t_N}\right) \widehat{\epsilon}_{m+q} & \cdots & B_1\left(\frac{t_{m+1+q}}{t_N}\right) \widehat{\epsilon}_{m+1} & \cdots & B_L\left(\frac{t_{m+1+q}}{t_N}\right) \widehat{\epsilon}_{m+1} \\ B_1\left(\frac{t_{m+2+q}}{t_N}\right) \widehat{\epsilon}_{m+q+1} & \cdots & B_L\left(\frac{t_{m+2+q}}{t_N}\right) \widehat{\epsilon}_{m+q+1} & \cdots & B_1\left(\frac{t_{m+2+q}}{t_N}\right) \widehat{\epsilon}_{m+2} & \cdots & B_L\left(\frac{t_{m+2+q}}{t_N}\right) \widehat{\epsilon}_{m+2} \\ \vdots & \ddots & \vdots & \ddots & \vdots & \ddots & \vdots \\ B_1\left(\frac{t_N}{t_N}\right) \widehat{\epsilon}_{N-1} & & B_L\left(\frac{t_N}{t_N}\right) \widehat{\epsilon}_{N-1} & & B_1\left(\frac{t_N}{t_N}\right) \widehat{\epsilon}_{N-q} & & B_L\left(\frac{t_N}{t_N}\right) \widehat{\epsilon}_{N-q} \end{matrix} \right)$$

Outline

Simulated LSAR(p) process

$p = 2$

$$Y_{i,N} = \alpha_1\left(\frac{t_i}{t_N}\right) y_{i-1,N} + \alpha_2\left(\frac{t_i}{t_N}\right) y_{i-2,N} + \varepsilon_{i,N}, \quad \{\varepsilon_{i,N}\} \overset{\text{iid}}{\sim} \mathcal{N}(0,1)$$

M=200 replications

$N = 100, 500, 1000$

B-splines of degree 3, $L = 7$

$t \overset{\text{iid}}{\sim} U[1, 1000]$

$\alpha_1(u) = 0.78 \sin(2\pi u),\ u \in (0, 1]$

$\alpha_2(u) = -0.4 \cos(\pi u),\ u \in (0, 1]$

Estimated parameters of the LSAR(2) process

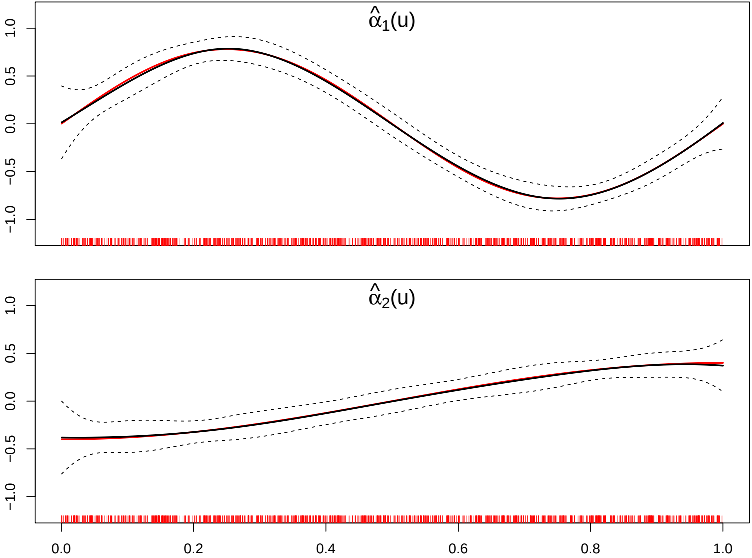

Simulated LSARMA(p,q) process

$p = q = 2$

$$Y_{i,N} = \sum_{j=1}^{2} \alpha_j\left(\frac{t_i}{t_N}\right) y_{i-j,N} + \varepsilon_{i,N} + \sum_{k=1}^{2} \beta_k\left(\frac{t_i}{t_N}\right) \varepsilon_{i-k,N}, \quad \{\varepsilon_{i,N}\} \overset{\text{iid}}{\sim} \mathcal{N}(0,1)$$

M=200 replications

$N = 1000, 5000, 10000, 20000$

In step 1: We fit a LSAR(6) model with B-splines of degree 1, and $L = 2$

In step 2: We fit a LSARMA(2) model with B-splines of degree 3, $L = 6$, and 5 iterations.

$t \overset{\text{iid}}{\sim} U[1, 1000]$

$\alpha_1(u) = 0.3\cos(3\pi u),\ u \in (0,1)$

$\alpha_2(u) = 0.6\sin(\pi u),\ u \in (0,1)$

$\beta_1(u) = -0.4u + 0.8u^2,\ u \in (0,1)$

$\beta_2(u) = -0.5\cos(2\pi u),\ u \in (0,1)$

Estimated parameters of LSARMA(2,2) process

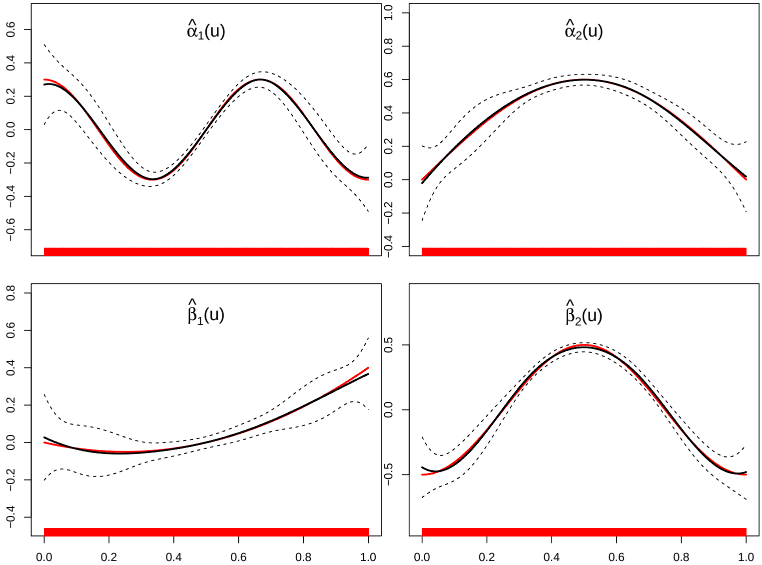

Outline

Data OGLE-LMC-LPV-00005

Kelly et al. (2014)

Data available at `https://github.com/brandonckelly/carma_pack`.

Description

435 observations

87% (380) observations in the training set

13% (55) observations in the forecasting set

Fit: CARMA(p, q) and LSAR(p) model

The (p, q) order of the CARMA model was chosen by AIC and BIC

The p order of the LSAR(p) model was chosen checking the residuals (correlation)

To fit the LSAR(p) model we consider B-splines of degree 3, knots as a sequence from 1 to 100 by 4 points, and λ between 0.01 and 1

Fit data OGLE-LMC-LPV-00005

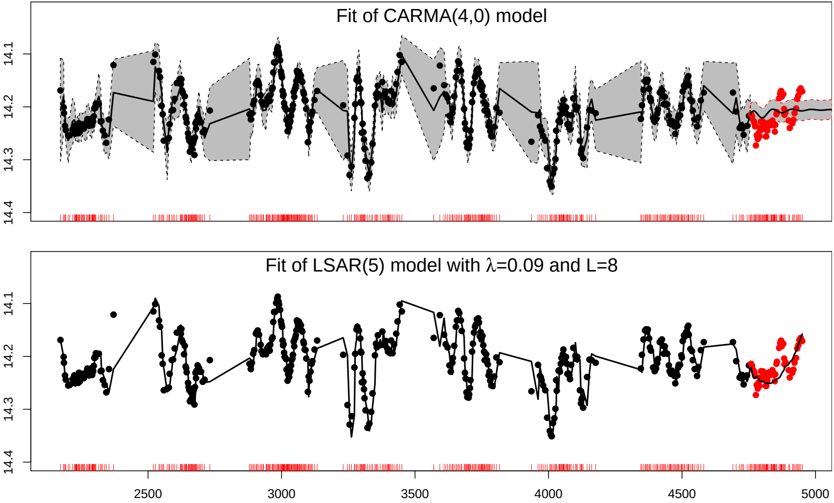

	CARMA(4,0)	LSAR(5)
training error	0.10534	0.15051
forecasting error	0.04548	0.03642

What do we learn?

So far

- The parameters of **Modulated**-Variable-Stars change over time
- Semi-parametric modeling where only part of the model depend on time (suitable for unequally spaced sampling)
- Parametric estimation helps handling missing obervations and improving forecasting accuracy

What's next

- Time-varying modes of the time-varying spectra
- Comparing/combining LS-ARMA vs C-ARMA.

Estimation of the time-varying spectral densities

Fully Non-parametric

$$\widetilde{\Sigma}(u,\omega) = \frac{2\pi}{h\,b\,T^2} \sum_{t,j=1}^{T} K_1\Big(\frac{u-\frac{t}{T}}{h}\Big) K_2\Big(\frac{\omega-\frac{\omega_j}{T}}{b}\Big) \widetilde{S}(t,\omega_j)$$

where $\widetilde{S}$ is the *pre-periodogram* (Neumann & Sachs, 1997)

$$\widetilde{S}(t,\omega) = \frac{1}{2\pi} \sum_{\ell : 1 \le [t+\frac{1}{2}\pm\frac{\ell}{2}] \le T} e^{-i\omega\ell}\; Y(\lfloor t+\tfrac{1+\ell}{2} \rfloor) Y(\lfloor t+\tfrac{1-\ell}{2} \rfloor)^*$$

Semi-parametric: TV-AR(p)

$$\widehat{\Sigma}(u,\omega) = \frac{\sigma_\varepsilon^2}{2\pi} \Big| \sum_{\ell=0}^{p} \widetilde{\alpha}_\ell(\tau)\, e^{i\omega\,\ell} \Big|^{-2}$$

Estimation of the time-varying spectral densities

Fully Non-parametric

$$\widetilde{\Sigma}(u,\omega) = \frac{2\pi}{h\,b\,T^2} \sum_{t,j=1}^{T} K_1\left(\frac{u-\frac{t}{T}}{h}\right) K_2\left(\frac{\omega-\frac{\omega_j}{T}}{b}\right) \widetilde{S}(t,\omega_j)$$

where $\widetilde{S}$ is the *pre-periodogram* (Neumann & Sachs, 1997)

$$\widetilde{S}(t,\omega) = \frac{1}{2\pi} \sum_{\ell: 1 \le [t+\frac{1}{2} \pm \frac{\ell}{2}] \le T} e^{-i\omega\ell}\, Y(\lfloor t + \tfrac{1+\ell}{2} \rfloor) Y(\lfloor t + \tfrac{1-\ell}{2} \rfloor)^*$$

Semi-parametric: TV-AR(p)

$$\widehat{\Sigma}(u,\omega) = \frac{\sigma_\varepsilon^2}{2\pi} \Big| \sum_{\ell=0}^{p} \widetilde{\alpha}_\ell(\tau)\, e^{i\omega\,\ell} \Big|^{-2}$$

two advantages:

- bandwidths to be selected only in time-domain
- forecasting becomes possible

In progress: with Malgosia Sobolewska

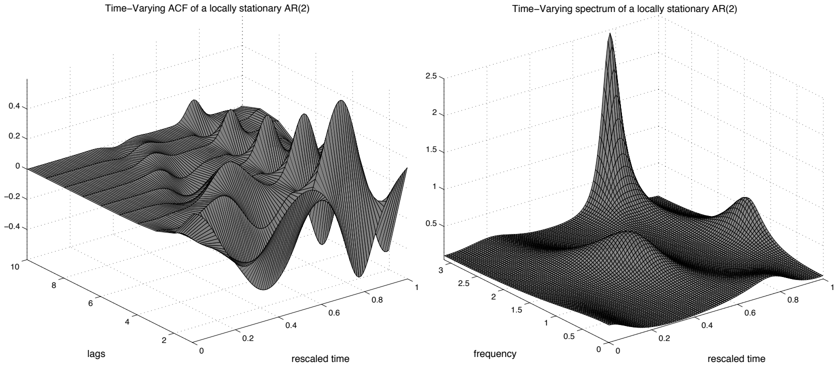

That's it

Thanks ☺